Forest Service
U.S. DEPARTMENT OF AGRICULTURE

Rocky Mountain Research Station RMRS-GTR-449 July 2025

Pollutant Emission Factors for Outdoor Recreational Fire Pits

Shawn P. Urbanski, Emily N. Lincoln, Stephen P. Baker, Bryce Nordgren, Larry Scott Baggett, Anne Jackson, Erica L. Belmont, and Luke P. McLaughlin

Urbanski, Shawn P.; Lincoln, Emily N.; Baker, Stephen P.; Nordgren, Bryce; Baggett, Larry Scott; Jackson, Anne; Belmont; Erica L.; McLaughlin, Luke P. 2025. **Pollutant emission factors for outdoor recreational fire pits**. Gen. Tech. Rep. RMRS-GTR-449. Fort Collins, CO: U.S. Department of Agriculture, Forest Service, Rocky Mountain Research Station. 74 p. https://doi.org/10.2737/RMRS-GTR-449

Abstract

Outdoor recreational wood burning, such as fire pit use, can produce large amounts of smoke that contains fine particulate matter (PM) and other air pollutants. Recently, purported “smokeless”, or low-smoke, fire pits have become widely available. Motivated by the apparent public desire for low-smoke options and the prospect of reducing PM pollution, the USDA Forest Service collaborated with the Minnesota Pollution Control Agency to measure air pollutant emissions from low-smoke fire pits. We measured emission factors (EF) for PM (EFPM), carbon monoxide, methane, and carbon dioxide for two low-smoke fire pits and a campground fire pit. Our study average EFPM = 2.2 (±1.1) g kg^{-1} (g of PM emitted per kg of dry firewood consumed; mean ± one standard deviation) is 80 percent lower than that used in the U.S. EPA National Emission Inventory (NEI), $EFPM_{NEI}$ (11.3 g kg^{-1}) for outdoor residential burning.

Implications: (1) the fire pits tested produce significantly less PM (per mass of firewood consumed) than traditional fire pits or fire rings, assuming the $EFPM_{NEI}$ reasonably characterizes the latter wood burning appliances; (2) the NEI may overestimate PM emissions from outdoor residential burning; and (3) applying our findings to the State of Minnesota indicates that replacing 25 percent of traditional fire pits with low-smoke versions could reduce the State’s annual PM emissions by approximately 1,300 metric tons.

Keywords: biomass burning, emission factors, air quality, fine particulate matter, recreational burning, fire pits, forest products, emission model

Cover: A scientist tests a lit fire pit. USDA Forest Service photo by Ian Grob.

Authors

Shawn P. Urbanski is a Research Physical Scientist with the Missoula Fire Sciences Laboratory, Rocky Mountain Research Station, U.S. Department of Agriculture, Forest Service in Missoula, Montana. (shawn.p.urbanski@usda.gov)

Emily N. Lincoln is a Chemist with the Missoula Fire Sciences Laboratory, Rocky Mountain Research Station, U.S. Department of Agriculture, Forest Service, in Missoula, Montana.

Stephen P. Baker is a Chemist with the Missoula Fire Sciences Laboratory, Rocky Mountain Research Station, U.S. Department of Agriculture, Forest Service, in Missoula, Montana.

Bryce Nordgren, Physical Scientist (retired) with the Missoula Fire Sciences Laboratory, Rocky Mountain Research Station, U.S. Department of Agriculture, Forest Service, in Missoula, Montana.

Larry Scott Baggett is a Statistician with the Rocky Mountain Research Station, U.S. Department of Agriculture, Forest Service, in Fort Collins, Colorado.

Anne Jackson is a Principal Engineer (retired) at the Minnesota Pollution Control Agency, in St. Paul, Minnesota.

Erica L. Belmont is an Associate Professor of Mechanical Engineering at the University of Wyoming, in Laramie, Wyoming.

Luke P. McLaughlin is a Graduate Research Assistant at the University of Wyoming, in Laramie, Wyoming.

Acknowledgments

This research was funded by the Minnesota Pollution Control Agency, under contract no. 19-CO-11221637-052 and U.S. Department of Agriculture, Forest Service Research & Development. Technical reviews by Madeleine Strum (USEPA) and Ashley Bittner (USEPA) are gratefully acknowledged.

This page intentionally left blank.

Contents

1. Introduction

Outdoor recreational burning is the use of chimineas, outdoor fireplaces, or fire pits in designated areas for cooking, pleasure, or ceremonial purposes. The popularity of outdoor recreational fires has been growing in recent years. In the 2018 Residential Landscape Architecture Trends Survey conducted by the American Society of Landscape Architects, 66 percent of the landscape architects surveyed expected fire pits/fireplaces to be among the features most requested by consumers (American Society of Landscape Architects 2018). The fire pit market size (in U.S. dollars) is predicted to grow at an annual rate of 5.6 percent from 2025 to 2030 (Grand View Research 2024).

We define outdoor recreational burning as outdoor burning of wood for recreational purposes including cooking, pleasure, or ceremony. This includes wood combustion in campfires, bonfires, and fire pits. Outdoor recreational burning can produce large amounts of smoke from incomplete combustion (Lemieux et al. 2004). The smoke from recreational burning, a complex mix of gases and fine particulate matter ($PM_{2.5}$; particulate matter with an aerodynamic diameter ≤2.5 μm), can easily be transported and can degrade local air quality. $PM_{2.5}$ is the pollutant in smoke that poses the greatest health risk to the public (USEPA 2023a). Outdoor recreational burning has no Federal regulation, but many State and local governments have instituted regulations for backyard usage, predominantly in urban areas. The National Emissions Inventory (NEI) compiled by the United States Environmental Protection Agency (USEPA) estimated the total national $PM_{2.5}$ emissions from residential outdoor burning devices (Source Classification Code (SCC) 2104008700) at approximately 53,100 mt (metric ton; 1 mt = 1000 kg) in 2020 (USEPA 2023b).

Purported “smokeless” (hereafter referred to as “low-smoke”) outdoor recreational fire pits became commercially available in the 2010s. The company Breeo began selling low-smoke fire pits in 2011, followed by the company Solo Stove in 2016. Most low-smoke fire pits have a similar design concept of creating a secondary combustion process with air circulating from a raised floor through a double-walled side cavity. The leading low-smoke fire pit companies are growing rapidly, indicating growing consumer demand. For example, Solo Stove sales increased from $16 million in 2018 to $130 million in 2020 (Huddleston and Rega 2023).

Motivated by an increase in outdoor recreational burning, the apparent consumer desire for low-smoke options, and possible highly localized air quality impacts, the United State Department of Agriculture (USDA) Forest Service Fire Sciences Laboratory (FSL) collaborated with the Minnesota Pollution Control Agency (MPCA) to measure air pollutant emissions from low-smoke fire pits. The State of Minnesota identified residential wood combustion, which includes stoves, boilers, fireplaces, and outdoor recreational equipment, as an important source of statewide $PM_{2.5}$ emissions (55% of the total) in 2014 (Kuhl-Stennes et al. 2019). An MPCA statewide survey of residential wood combustion estimates that outdoor recreational equipment burned 430,000 cords of wood over the 2020–2021 heating season, which accounts for 28 percent of the wood burned statewide (Kuhl-Stennes et al. 2022).

The objective of this project was to determine if self-advertised low-smoke fire pits produce less $PM_{2.5}$ than traditional fire pits, and if so, evaluate the potential of reducing PM pollution by replacing traditional fire pits with the low-smoke variety. To achieve this objective, we designed a study to quantify $PM_{2.5}$ emission factors for two low-smoke fire pits and a campground fire pit and then used the test data to create a model for estimating emissions from annual inventories of firewood use. The $PM_{2.5}$ emission factors were quantified for each fire pit based on emissions measured during a burn cycle designed to represent a typical recreational fire. An emissions model was used to estimate annual $PM_{2.5}$ emissions from low-smoke recreational fire pits in the State of Minnesota using an MPCA statewide firewood use survey.

Over the three rounds of testing, split firewood of different moisture content (MC) levels was burned in 31 burns during which emissions of $PM_{2.5}$ and PM_1 (PM with an aerodynamic diameter ≤ 1.0 μm), carbon dioxide (CO_2), carbon monoxide (CO), and methane (CH_4) were measured. Measurements of CO_2 and CO were used to determine modified combustion efficiency (MCE) and emission factors (EF) for CO_2, CO, CH_4, and PM. (Hereafter we will use PM to refer to $PM_{2.5}$ and PM_1 for reasons discussed in the *Methods* section.) In the third round of testing, the size distribution of particles was also measured for three of the burns.

2. Methods

2.1 Combustion Facility

The fire pit testing was conducted in the FSL combustion chamber, which is depicted in figure 1. The combustion chamber measures 12.5 m × 12.5 m × 22 m high. An exhaust stack with an inverted funnel at its entrance extends from 2 m above the floor to the top of the chamber. A sampling platform surrounds the stack 17 m above the chamber floor. The funnel opening of the exhaust stack is 3.5 m diameter and the exhaust stack is 1.6 m diameter. Air from outside the building enters the chamber through vents near the floor along the walls and is drawn through the stack, entraining emissions from fires burning directly beneath the funnel. The linear flow rate within the exhaust stack was about 1.8 m s^{-1} at the sampling platform. Within the exhaust stack, a few meters from the funnel opening, is a diffuser ring (0.8 m inside diameter) which mixes the air and entrained emissions. At the height of the sampling platform temperature and concentrations of gases in smoke are uniform across the width of the stack (Christian et al. 2004). During our testing, gas and particle measurement equipment was positioned on the platform and the emissions were drawn through sample lines constructed of stainless steel, Teflon, or conductive tubing as described in section 2.6.

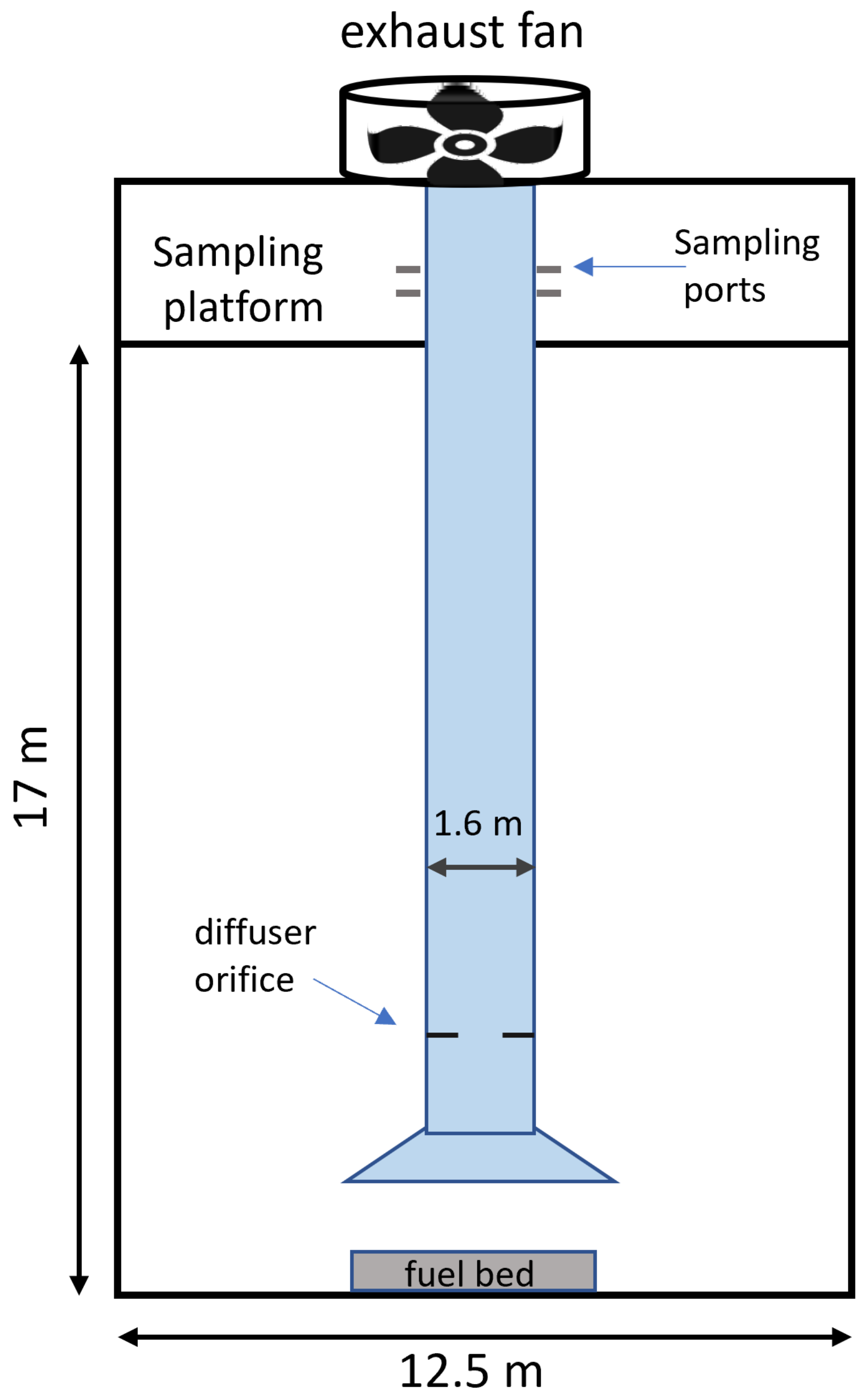

Figure 1—Schematic of the USDA Forest Service Fire Sciences Laboratory (FSL) combustion chamber.

2.2 Fire Pits Tested

Two widely available outdoor fire pits designed to burn cordwood (wood logs, i.e. firewood cut and split into conveniently sized pieces for easy stacking into cords) with minimal smoke production (low-smoke), the Solo Yukon Stove (Solo) and the Breeo X Series 24 (Breeo), and the Pilot Rock FSW-24/18/PA Accessible Campfire Ring (Pilot), an Americans with Disabilities Act compliant campfire ring, were tested. Photos of the fire pits and dimensions are provided in figure 2. The Pilot fire pit was filled with 20 cm of sand to raise the burn area to the manufacturer's specifications. The approximate useable volumes of the fire pits were 0.16 m^3 for the Solo, 0.12 m^3 for the Breeo and 0.13 m^3 for the Pilot (after filling with 20 cm of sand). The Solo and Breeo fire pits included instructions for wood log loading which were followed as closely as possible during the testing. Both the Solo and Breeo fire pits instructed that wood logs be kept below the interior ventilation holes (fig. 2), which was done throughout the testing. Instructions with the Solo and Breeo fire pits and online instructions (including video guides) were used to ensure the fire pits were operated as intended by the manufacturer. We note that in the time since testing, both Solo and Breeo have introduced additional fire pit models.

2.3 Fuels

Pallets of firewood—a mix of northern red oak, maple, and birch from Minnesota—were used in the fire pit testing. The firewood had typical dimensions of 15 inches in length and a cross section of 3 inches (fig. 3). Firewood used in the first two rounds of testing was delivered to the FSL (Missoula, MT) in April of 2019. Half of this firewood load was conditioned at ambient conditions prior to tests in May 2019. The remaining firewood was cured for nine months (April–December) at ambient conditions (while shielded from precipitation) for testing emissions from low-moisture-content firewood in December 2019. A third round of tests used firewood delivered to the FSL several weeks before the June 2021 tests.

Figure 2—Fire pits post testing. (A) Solo, (B) Breeo, and (C) Pilot. Fire pit heights (H), diameters (D), and volumes (V) are Solo: H = 43 cm (17 inch), D = 69 cm (27 inch), V = 0.16 m^3 (5.6 ft^3); Breeo: H = 41 cm (16 inch), D = 61 cm (24 inch), V = 0.12 m^3 (4.2 ft^3); Pilot: H = 46 cm (18 inch), D = 81 cm (32 inch), V = 0.13 m^3 (4.6 ft^3) after accounting for 20 cm of sand (see section 2.2).

Figure 3—Firewood used in testing. (A) Split firewood log, (B) split log, (C) face cord of split firewood, and (D) firewood being conditioned in the FSL environmental chamber.

During fire pit testing, the moisture content of the firewood was determined by periodically splicing a lengthwise sample of wood, with a maximum width of roughly one to two inches, from a log immediately prior to its addition to the fire pit. Approximately four to eight moisture samples were collected per burn. This sampling technique may underestimate the total moisture content of the log. The mass of the wood sample, W_s, was immediately measured and recorded. The wood samples were then oven dried at 90 °C for 24 to 48 hours and reweighed to determine their oven-dry mass, W_o. The moisture content as percent of the wood dry mass (dry-weight mass), MC, was then calculated as $MC = ((W_s - W_o)/W_o)*100$. During the fire pit testing the burn average MC for each round was 10–27 percent (May 2019, round 1), 6–9 percent (December 2019, round 2) and 14–35 percent (June 2021, round 3). The MPCA recommends only burning wood with an MC of less than 20 percent (Kuhl-Stennes et al. 2022).

2.4 Burn Procedure

The burn cycle used for emission testing consisted of three phases: burnup, steady, and burndown. The steady phase represents the standard mode of recreational use—maintenance of a robust fire through periodic additions of split logs. The purpose of the burnup phase was to initiate a robust, steady fire. In the burnup phase, the ignition fuel bed was a small amount of excelsior shavings (<100 g), several pieces of kindling spliced from split logs, and one or two split logs. Following ignition, logs were added to the fire, at semi-regular intervals over a period of 20–30 minutes. The steady phase began after a regular, consistent fire was achieved. During the steady phase logs were added at a regular interval of about 10 minutes over a period of 45–60 minutes. Each log addition during the steady phase was one to three logs, with the number added varied as needed to maintain a robust fire. In practice, the steady phase may last several hours; however, in our testing only about 45 minutes was required to characterize pollutant emissions. During the burnup and steady phases, the masses and log count for all wood additions were recorded. The burndown phase was a 20–30-minute period beginning 10 minutes after the final steady phase log addition.

At the end of the burndown phase the fire was extinguished with water to preserve charcoal, ash, and unburnt firewood. The charcoal, ash, and unburnt wood were allowed to air dry for around 24 hours before being removed from the fire pit and transferred to heavy-duty aluminum trays. Through a combination of air drying, exposure to sun, and placement in ovens, the charcoal, ash, and unburned wood were dried over several days and then weighed to determine the dry-weight mass of the unconsumed firewood. The dry-weight mass of firewood consumed over an entire burn (FC) was calculated as difference in the dry-weight mass of the firewood input and the charcoal, ash, and unburnt wood remaining after the fire. Combustion completeness (CC), the mass fraction of firewood consumed over an entire burn, was calculated as the dry-weight mass of firewood consumed (FC) divided by the dry-weight mass of firewood input (table 1). Photos of typical fire behavior during the burn phases are shown in figure 4.

Table 1—Summary of test burns. Moisture content is percent of dry mass. Firewood input, firewood consumed, and ash and charcoal are reported as dry mass. The fraction of firewood consumed is the burn total combustion completeness (CC).

BurnID	Round	Date	Firepit	Firewood MC (percent)	Firewood Raw Mass (g)	Firewood Input (g)	Ash and Charcoal (g)	Firewood Consumed (g)	Firewood Consumed (percent)
2019050803	1	20190508	Solo	27	30227	23726	1262	22464	95
2019050804	1	20190508	Breeo	21	27372	22697	3460	19237	85
2019050905	1	20190509	Breeo	24	28492	22904	4097	18807	82
2019050906	1	20190509	Solo	11	30141	27081	2084	24997	92
2019051007	1	20190510	Breeo	13	24865	21966	3337	18629	85
2019051008	1	20190510	Solo	14	33638	29611	3270	26341	89
2019051309	1	20190513	Breeo	10	24174	21956	2922	19034	87
2019051310	1	20190513	Pilot	18	23302	19681	3314	16367	83
2019051411	1	20190514	Pilot	14	25368	22233	4363	17870	80
2019120901	2	20191209	Breeo	9	29213	26801	3660	23141	79
2019121002	2	20191210	Breeo	9	30648	28117	4481	23636	77
2019121103	2	20191211	Solo	7	32245	30136	2272	27864	86
2019121104	2	20191211	Solo	6	35836	33808	2200	31608	88
2019121205	2	20191212	Solo	8	37232	34474	3470	31004	83
2019121306	2	20191213	Breeo	8	27208	25193	4559	20634	76
2019121607	2	20191216	Pilot	8	27570	25528	3776	21752	79
2019121708	2	20191217	Pilot	8	30086	27857	n.m.[a]	22007[b]	79[b]
2019121809	2	20191218	Solo	9	29464	27031	2215	24816	84
2019121910	2	20191219	Breeo	8	28556	26441	4983	21458	75

a n.m. = not measured.

b The ash pit, which was left to cool overnight, was not fully extinguished and smoldered overnight preventing an accurate measurement of post burn ash. It was assumed the percent consumption for this burn was the same as that for the other Pilot burn for this round of testing (79%).

Table 1 continued.

BurnID	Round	Date	Firepit	Firewood MC (percent)	Firewood Raw Mass (g)	Firewood Input (g)	Ash and Charcoal (g)	Firewood Consumed (g)	Firewood Consumed (percent)
2021060701	3	20210607	Breeo	28	31123	24315	7639	16676	69
2021060802	3	20210608	Breeo	35	31142	23068	10577	12491	54
2021060903	3	20210609	Solo	24	31628	25506	7070	18436	72
2021061004	3	20210610	Solo	25	30603	24482	7442	17040	70
2021061105	3	20210611	Solo	14	31022	27212	6778	20434	75
2021061506	3	20210615	Breeo	21	31315	25880	7084	18796	73
2021061507	3	20210615	Solo	30	31118	23937	5621	18316	77
2021061708	3	20210617	Breeo	27	31455	24768	6949	17819	72
2021062109	3	20210621	Pilot	19	31617	26569	5894	20675	78
2021062110	3	20210621	Pilot	17	32624	27884	7617	20267	73
2021062211	3	20210622	Pilot	23	32702	26587	15781	10806	41
2021062312	3	20210623	Pilot	26	32365	25687	13838	11849	46

Figure 4—Burn phases of fire pit testing: (A) burnup phase, (B) steady phase, and (C) burndown phase.

2.5 Laboratory Setup

The experiment setup on the combustion chamber floor is shown in figure 5, and instruments deployed on the chamber floor and sampling platform are listed in table 2 and described in section 2.6. The fire pit being tested was placed directly under the center of the exhaust stack (fig. 5). Two radiant heat sensors were placed a horizontal distance of 0.7 m (2.3 ft) from the fire pit center and vertically positioned approximately 10 cm (3.9 in) above the fire pit rim (fig. 5). The inlet of a CO_2 gas analyzer (LI-COR LI-7000), which was used to monitor the background CO_2 concentration, was placed 130 cm (51.2 in) from the fire pit center at a height of 90 cm (35.4 in) above the chamber floor.

On the sampling platform (fig. 1) a cavity ring-down spectroscopy (CRDS) gas analyzer sampled emissions from the exhaust stack through lines constructed of Teflon. Particulate matter filter sampling units and a three wavelength nephelometer (during rounds 1 and 2) were positioned on the platform and the emissions were drawn from the exhaust stack through sample lines constructed of stainless steel and conductive tubing. During the final five burns of round 3 testing, the LI-COR CO_2 gas analyzer was repositioned to the sampling platform as a backup measurement for the CRDS analyzer, which began having computer hardware issues that resulted in periodic failure to log data (section 3). The chamber floor (background) CO_2 measurements obtained in the previous 24 burns showed that fluctuations in the background CO_2 over the duration of a burn were negligible for characterizing emissions. Based on this CO_2 background stability demonstrated by the LI-COR measurements, we used the background CO_2 as measured in the stack over 10 minutes immediately prior to the start of each burn.

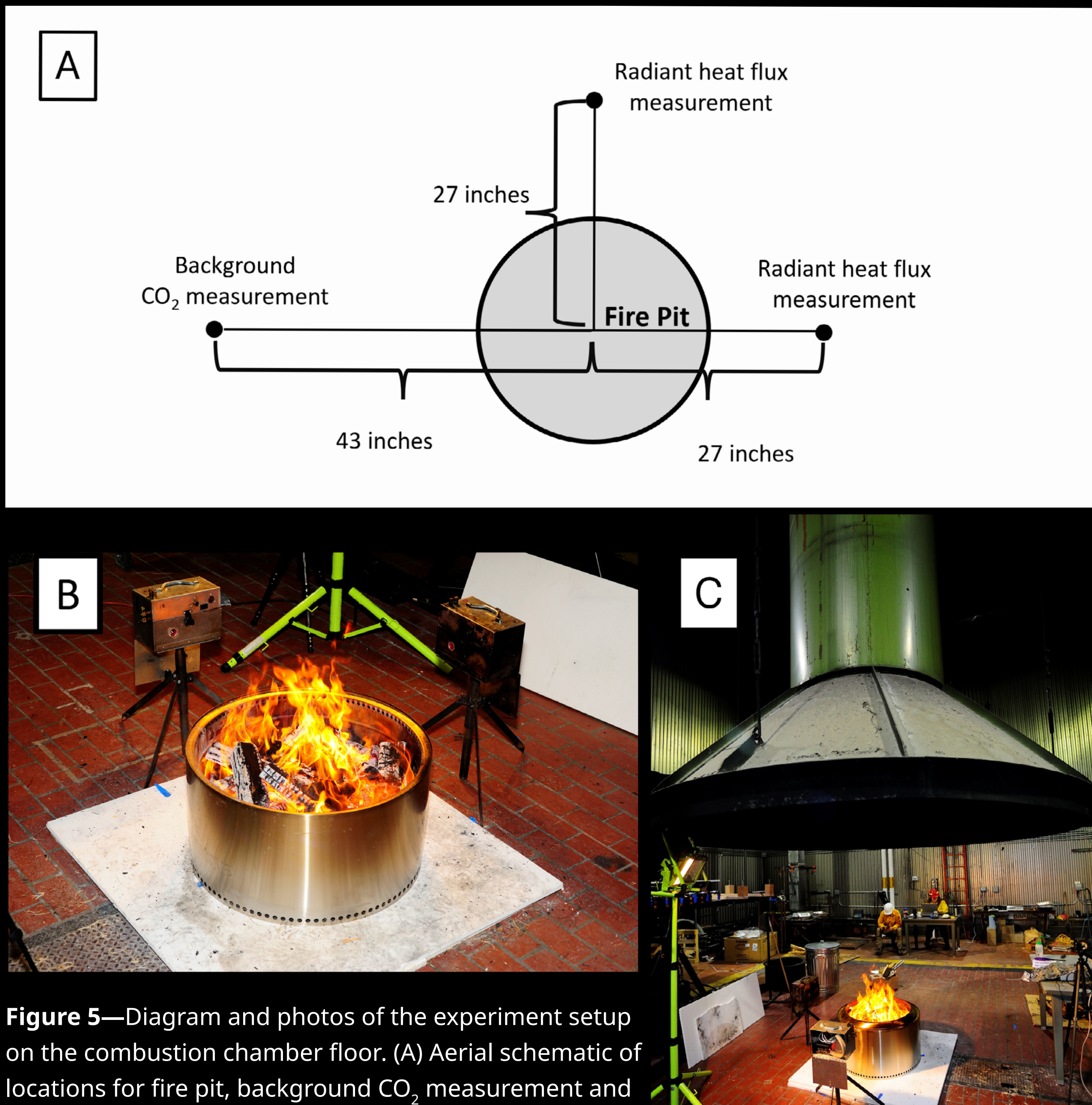

Figure 5—Diagram and photos of the experiment setup on the combustion chamber floor. (A) Aerial schematic of locations for fire pit, background CO_2 measurement and radiant heat measurements. (B) The Solo fire pit during testing. (C) The Solo fire pit and combustion chamber exhaust stack during testing. USDA Forest Service photos.

Table 2—Instrumentation.

Measurement	Round	Method	Instrument	Details
CO_2, CO, CH_4, H_2O	1, 2, 3	Cavity Ring-Down Spectroscopy	Picarro G2401-m	2 s rate
PM_1	1	Gravimetric analysis, 37 mm Teflon filter	UGR cyclone, 1 um cutoff	14 slpm, 20-30 min sample
$PM_{2.5}$	2, 3	Gravimetric analysis, 47 mm Teflon filter	ARA Instruments LFR-6, 2.5 µm cutoff impactor	6 slpm, 20-30 min sample
Total light scattering (bsct)	1, 2	Light scattering at 700, 550, 450 nm	TSI integrating nephelometer Model 3563	0.5 s rate
Particle size distribution	3	Electrical low-pressure impactor, 14 stages 10 nm to 10 µm	Dekati HT-ELPI+ Model 2E10-10	1 Hz rate, aggregated to 10-minute windows
Radiant heat flux (RF)	1, 2, 3	Schmidt-Boelter Thermopile and Gardon Sensors	Medtherm Dual Sensor Heat Flux sensors (Model 64-20T)	10 Hz, black body calibration 0 - 200kW m^{-2}
CO_2	1, 2, 3	Non-Dispersive Infrared Absorption	LI-COR LI-7000	1 Hz

2.6 Instrumentation

The instrumentation used in the testing is listed in table 2. Detailed descriptions of the instruments and their uses are found in the following subsections.

2.6.1 Particulate matter—

In rounds 2 and 3, PM emissions ($PM_{2.5}$) were measured using an ARA Instruments Low Flow Research Sampler (LFR-6) configured for stack sampling. The accuracy of the ARA sampler for measuring mass concentrations of $PM_{2.5}$ in biomass burning smoke was verified against a Tisch Federal Reference Method (FRM) monitor in collaboration with the USEPA in a series of static chamber burns at the FSL in April 2019 (Krug et al. 2021). The sampler pulled emissions through stainless steel tubing inserted 60 cm into the exhaust stack. The sampler drew emissions at 6 slpm (standard liters per minute) from the exhaust stack through an FRM style impactor with a cutoff of ≤2.5 µm aerodynamic diameter and onto a 47 mm Teflon filter. During round 1 testing, PM emissions (PM_1) were collected by pulling emissions from the exhaust stack through a conductive tubing sample line connected to a copper tube inserted 60 cm into the exhaust stack at 14 slpm through a cyclone with a cutoff of ≤1.0 µm aerodynamic diameter (URG-2000-30EC, URG Corp., USA) and onto a 37 mm Teflon filter.

The literature on biomass burning PM shows most fine particulate matter mass ($PM_{2.5}$) in fresh smoke is contained in submicron particles (PM_1) (Hosseini et al. 2010; Reid et al. 2005), thus for our emissions testing $PM_{2.5}$ and PM_1 mass concentration measurements are roughly equivalent. For this reason, we report $PM_{2.5}$ and PM_1 as PM, fine particulate matter. Particle size distribution measurements taken for three burns during round 3 testing confirmed that particle numbers and mass were minimal for particle diameter >1µm (section 3.2).

One or more Teflon filter samples were collected during each fire phase. The 37 mm and 47 mm Teflon filters used in the PM determination were conditioned and weighed in a controlled-environment room at 68 °F and 35 percent (±5%) relative humidity. Prior to weighing, the filters were conditioned for at least 24 hours. Polonium-210 (210Po) antistatic strips were used immediately before the weighing process to reduce the interference of static electricity buildup. Each filter was weighed three times on a Mettler M4 microbalance with a precision of 1.0 µg. The balance was linked to a software program that collects and stores the weights and room condition. The balance was tared (zeroed) before each weighing. A calibration weight was used once every five filters to verify the accuracy and calibration of the microbalance. Filters whose weights were not reproducible to within 5 µg were withheld from analysis. One control filter per day, handled in the same manner as the treatment filters, was used to correct for environmental and handling variability in the filter weights. Each filter was pre-weighed prior to sample collection using this procedure, and then again after emission sampling.

For post-emission sampling, the filters were again conditioned at least 24 hours to stabilize the particulate matter weights. The PM concentrations were calculated based on the final particulate matter weights (post-weight minus pre-weight plus change in control filter mass (if any)), and the volume of air drawn through the filter during the emissions sampling. During fire pit testing, at the end of each day the filters with samples were placed in a freezer to preserve semi-volatiles that may evaporate over time. The filters were analyzed using the methods described above within one week after completion of the fire pit testing.

During round 3 testing, visiting researchers from the University of Wyoming measured particle size distributions for three burns. Particles were sampled from the center of the burn chamber stack at a rate of 2.7 slpm using a rotary vane vacuum pump and 0.25 inch inside-diameter stainless steel tubing. The aerosol stream was then diluted with 4.0 slpm of dry air and the diluted mixture was drawn at a total rate of 6.7 slpm into an electrical low-pressure impactor (ELPI by Dekati) for real-time aerosol number and size measurement. The ELPI has 14 detection stages covering particle sizes 10 nm to 10 µm. The measurements consistently showed minimal particle count and mass for particle diameter >1 µm (section 3.2.2).

2.6.2 CO_2, CO, and CH_4—

Continuous measurements (data acquisition rate 2 s) of CO_2, CO, and CH_4 were obtained using a CRDS trace gas analyzer (G2401-m, Picarro Inc., USA). Details of the CRDS method and this specific instrument may be found elsewhere (Urbanski 2013). Air was sampled by the CRDS through Teflon tubing connected to stainless steel tubing inserted in the exhaust stack with its orifice near the stack's center. A three-point calibration was run periodically to verify the accuracy of the CRDS measurements. Gas mixtures of CO_2, CO and CH_4 in Ultrapure air served as calibration standards. The CRDS response varied little from day to day and the study average calibration factors were applied to the data offline. A LI-COR CO_2 analyzer was used to monitor the background CO_2 on the chamber floor and was cross calibrated versus the CRDS analyzer.

2.6.3 Nephelometry—

A TSI three wavelength integrating nephelometer (table 2) was used in testing rounds 1 and 2 to measure total light scattering at 700 nm (red), 550 nm (green), and 450 nm (blue) at a data acquisition rate of 0.5 Hz. Total light scattering at these wavelengths responds strongly to PM concentration, particle size distribution, and particle composition. The nephelometer measurements may be used to estimate the temporal PM concentration profile based on the integrated PM measurements obtained with the filter sampling system.

2.6.4 Radiant Heat—

Radiant energy flux was measured using Medtherm Dual Sensor Heat Flux sensors (table 2) contained in Fire Behavior Packages (FBP). The FBP have been widely used in field research projects conducted by the FSL's fire behavior research group, and details may be found in (Jimenez et al. 2007). The heat flux sensors were calibrated in a black body over a range of 0 to 200 kW m^{-2} and fit a power law curve to the calibration data.

2.7 Emission Calculations

Emissions of species X per kg of firewood consumed (dry-weight mass) were quantified using burn phase average excess mass mixing ratios ΔX ($\Delta X = X_{smoke} - X_{background}$). Phase average emission factors for each species X, EFX, were calculated using the carbon mass balance method (USEPA 2022) implemented with equation 1. In equation 1, ΔC_i are the excess mass mixing ratios of carbon in species X (mg C mg air^{-1}), and F_c is the mass fraction of carbon in the dry fuel which was taken as 0.50 for all wood used in this study.

$$EF_x = F_c \times 1000\left(g\ kg^{-1}\right) \times \frac{\Delta X}{\Delta C_{CO_2} + \Delta C_{CO} + \Delta C_{CH_4} + \Delta C_{PM}} \quad (1)$$

The carbon mass balance method assumes that all fuel carbon volatilized as gases or PM is measured. However, since the majority of carbon (more than 95%) in fresh biomass smoke from efficient fires is contained in CO_2, CO, and CH_4 (Urbanski 2014), neglecting other carbon containing gases in the carbon mass balance method introduces only a minor positive bias of less than 5 percent. The steady phase of the testing was highly efficient, the fraction of measured carbon in species other than CO_2 was quite small, and the EFPM calculated using only carbon from ΔCO_2 and ΔPM in the denominator of equation 1 resulted in a less than 5 percent overestimate compared to EFPM calculated using all four species. We assumed a PM carbon content of 75 percent (Reid et al. 2005) in our EF calculations. The difference in the denominator between an assumed PM carbon content of 0 percent and 100 percent was <1 percent. In biomass burning, modified combustion efficiency (MCE; $MCE = \Delta CO_2/(\Delta CO_2 + \Delta CO)$) is often used to characterize the relative amount of flaming and smoldering combustion (Akagi et al. 2011). The MCE approaches 0.99 for “pure” flaming combustion (Yokelson et al. 1996).

Firewood consumption (dry-weight mass) by fire phase, FCi, was calculated using equation 2:

$$FC_i = FC \times \frac{\Delta C_i \times \Delta t_i}{\sum \Delta C_i \times \Delta t_i} \quad (2)$$

In equation 2 the index *i* is the fire phase (burnup, steady, burndown), *FC* is the dry-weight mass of firewood consumed over the entire fire (g; table 1), FC_i is the dry-weight mass of firewood consumed in phase i, ΔC_i is average mass mixing ratio of carbon (mg C mg air^{-1}) emitted during phase i (denominator of equation 1), and Δt_i is the sampling duration of phase i (s). The FC is the total firewood consumed during each burn and is the dry-weight mass difference between the firewood input and postburn ash, charcoal, and unburnt wood (table 1). The continuous time-series measurements of gaseous carbon emissions (ΔC) were used to partition burn total firewood consumption across the burn phases (equation 2), as illustrated in figure 6.

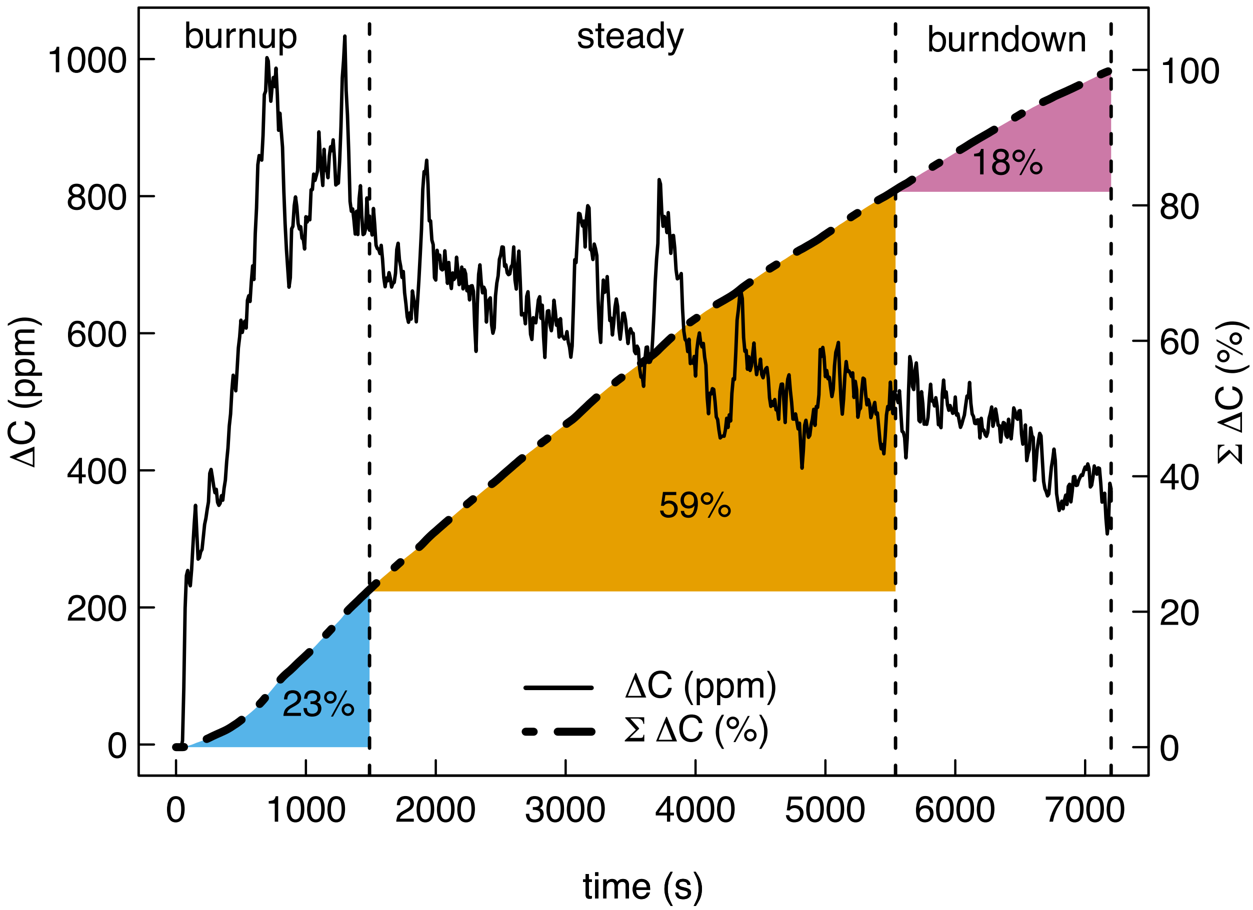

Figure 6—Time series of concentration of carbon emitted as 10-second averages (solid black line; ΔC) and cumulative sum of carbon emitted as percent of total emissions (dashed black line; ΣΔC) for BurnID 2019121002 (Breeo fire pit). The carbon emitted is proportional to the mass of firewood consumed. In this burn, carbon emission, and hence firewood consumption, by burn stage was burnup = 23%, steady = 59% and burndown = 18%.

2.8 Statistical Methods

The primary goal of our study is to provide one set of parameters for estimating pollutant emission inventories from low-smoke outdoor recreational wood burning fire pits at firewood moisture content (MC) values of 10 percent to 30 percent. This parameter set, which represents the average low-smoke fire pit, consists of burn phase (burnup, steady, and burndown) specific pollutant emission factors (EFPM, $EFCH_4$, EFCO, $EFCO_2$) and firewood combustion completeness (CC; defined as the dry-weight mass fraction of firewood consumed in the fire, see section 2.4). To achieve this goal, we employed multiple generalized linear mixed models (GLMMs) in which EFX and CC were the response variables, and firewood moisture content and fire pit type were the predictor variables.

Of the three fire pit types tested, the Pilot, an ADA accessible campground fire pit, is not advertised as a low-smoke appliance. However, the three fire pits have a similar barrel shaped design that promotes secondary combustion and similar dimensions (section 2.2) and produced similar PM emissions (section 3). Based on the large body of literature on the burning rates, consumption, and pollutant emissions from wildland fuel combustion (Urbanski et al. 2022), it was anticipated that EFs and CC will depend on MC in the burnup and steady burn phases.

All EFs and CC were modeled by burn phase using a GLMM approach that included main effect predictors of fire pit type and moisture content (MC) and fire pit type–MC interaction. Response CC was modeled assuming a beta distribution with a logit link function because the response domain was restricted to the open interval (0,1). Responses EFPM, $EFCO_2$, EFCO and $EFCH_4$ were modeled assuming gamma distributions with log-link functions because the response domains were restricted to the open interval $(0, \infty)$. All models included separate dispersion parameters to account for response heterogeneity among the fixed effects. Model adequacy was validated using simulation tests for under/over dispersion using R library DHARMa (Hartig 2022). Treatment contrasts were adjusted for family-wise experiment rate using Tukey's HSD method (Kramer, 1956). Data were analyzed using the R statistical environment version 4.4.1 (R Core Team, 2024) and R libraries glmmTMB (Brooks et al., 2017) and emmeans (Lenth, 2024).

3. Results

A total of 31 burns were conducted as summarized in table 1. The course of a typical burn is illustrated by figure 7 which shows time-series of gaseous carbon emissions (ΔC), modified combustion efficiency (MCE), radiant heat flux (RF), particle light scattering (bsct), and firewood input for firewood burned in the Breeo (BurnID = 2019121002; see table 2). Following ignition and during the first few rounds of firewood addition, RF remains low (<200 W m^{-2}) and gaseous carbon emissions (ΔC) are less than half the average value of the steady phase (fig. 7). By the end of the burnup phase ΔC peaked, and RF has neared the average value measured over the steady phase. Rapid increases in particle concentrations (indicated by bsct) follow inputs of firewood (fig. 7). During the later portion of the burnup phase and throughout the steady phase, inputs of firewood produced a large spike in ΔC, while RF spikes upon firewood addition do not occur consistently. During the burndown phase, MCE decreases rapidly (fig. 7) due to a shift in production of CO_2 to CO. The increase in CO production during the burndown phase was coincident with the transition to glowing combustion of char which is characterized by low MCE and relatively high EFCO (Yokelson et al. 1996). While peak ΔC concentrations were seen during the burnup phase, when firewood was added rapidly (fig. 7) to initiate a steady and robust fire, most firewood was consumed during the steady phase (fig. 7).

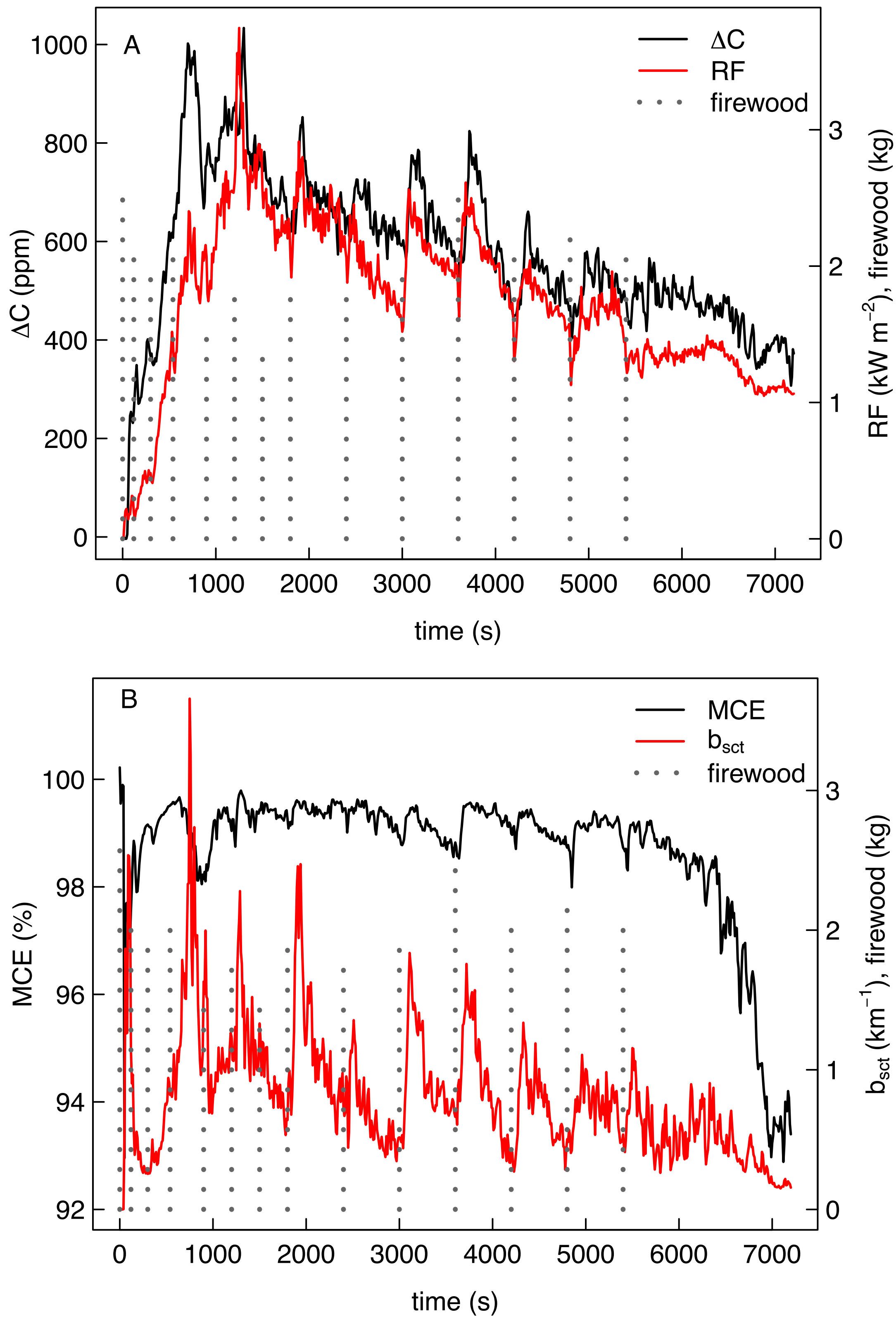

Figure 7—Data time series for a typical burn (Breeo fire pit, burnid 2019121002). (A) Carbon emitted (ΔC), radiant heat flux (RF), and firewood inputs; and (B) modified combustion efficiency (MCE), light scattering (bsct), and firewood inputs.

Firewood input, consumption, and MC for the 31 tests are summarized graphically in figure 8 by test round. Across all tests 803 kg of firewood was used and the median input and consumption were 25.7 kg and 20.3 kg, respectively. Firewood MC ranged from 6 percent to 35 percent with a median of 14 percent. Round 2 testing, which used well-cured firewood, had the lowest MC, with a median equal to 8 percent and the highest firewood input and consumption. As will be discussed in later sections, MC had a noticeable influence on the amount of fuel consumption, especially at the low MC range tested in round 2. Over the three rounds the number of successful tests per fire pit were 11 for Solo, 12 for Breeo, and 8 for Pilot (table 1).

During round 3 of testing, a recurring software malfunction resulted in periodic losses of CRDS data (CO_2, CO, CH_4), affecting five burns. Figure 9 shows the percentage of CRDS data lost by burn phase. Virtually no data was lost during the burnup phase because the software was restarted prior to each burn and the malfunction typically surfaced after approximately 25 minutes or more of operation. The malfunction subsided for the final two burns of round 3 testing. To partially cover for the periodic CRDS data losses, the LI-COR CO_2 instrument was redeployed to the sampling platform for the final five burns of round 3 testing. The LI-COR was calibrated versus the CRDS, and its measurements were used to gap fill missing CRDS CO_2. The LI-COR data allowed us to calculate EFPM using carbon from PM and CO_2 only (EFPM*) with CRDS data gaps filled as needed. For the 26 burns with complete CRDS data, the difference between EFPM* and EFPM is minimal. We found that for the steady and burndown phases EFPM* overestimates EFPM by approximately 5 percent and 7 percent, respectively (see Appendix A, fig. A.1). Thus, substituting EFPM* for EFPM for the five burns where the steady and burndown fire phases were missing CRDS data will introduce only a small positive bias.

In the following subsections, after summarizing measurements of EFs and firewood input (FW) and consumption (FC) according to burn phase, the discussion of results is centered on the GLMMs of EFs and CC (section 2.8). Our primary goal is to provide parameters for estimating pollutant emissions from the average low-smoke fire pit. Therefore, we focus on the GLMMs' MC main effects—the burn phase specific response of EFs and CC to MC averaged across the three fire pit types. However, to provide insight into possible differences between the fire pits, we also discuss the GLMMs' fire pit type main effects and fire pit type–MC interactions. In section 4, the results are used to develop a model for estimating PM emission inventories for low-smoke fire pits from firewood use activity data.

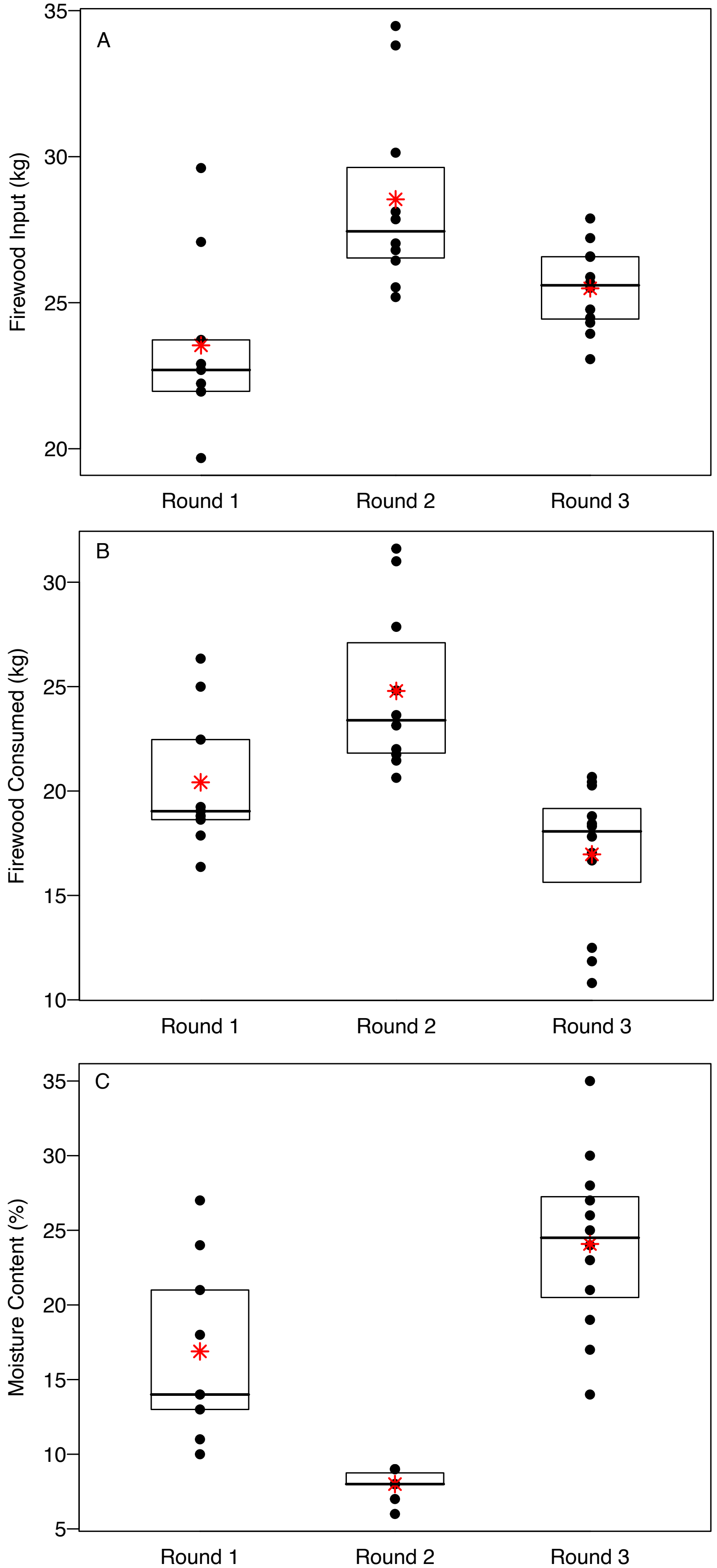

Figure 8—(A) Firewood input, (B) firewood consumed, and (C) firewood moisture content by test round (table 2). Median (thick black line), lower and upper quartiles (box), mean (red stars), and individual values (filled circles).

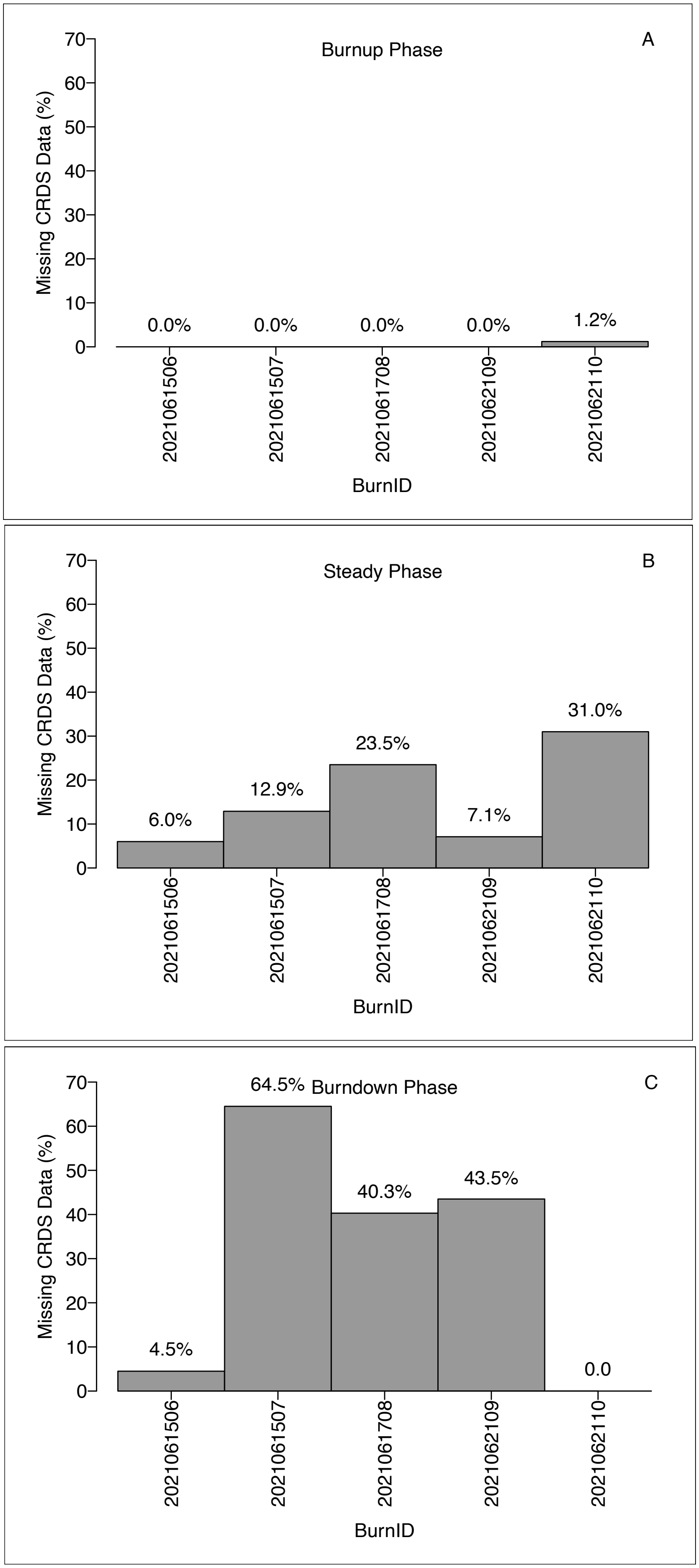

Figure 9—The percentage of CRDS data lost due to software malfunctioning during the third round of testing. (A) Burnup phase, (B) steady phase, and (C) burndown phase.

3.1 Pollutant Emissions

The EF are summarized by burn phase in figure 10 and table 3. Individual results for all 31 burns are provided in Appendix B. The study average EFPM decreased by phase, being greatest during the burnup phase and lowest for the burndown phase. However, this pattern did not hold for every individual burn. Study average burnup phase EFPM was about 60 percent higher than that of the steady phase. For biomass burning, EFPM is usually negatively correlated with MCE; however, the burnup and steady phase MCE are similar (table 3), indicating the difference in EFPM is not a simple result of differences in combustion efficiency. The trend in study average $EFCH_4$ across burn phases was opposite that of EFPM, with the burndown phase $EFCH_4$ being roughly twice that of the burnup phase. For study average EFCO, the burndown phase was more than twice that of the burnup or steady phases. Study average $EFCO_2$ trended opposite that of EFCO. The relatively high EFCO and low $EFCO_2$ during the burndown phase is consistent with this phase being dominated by glowing combustion of char (Yokelson et al. 1996).

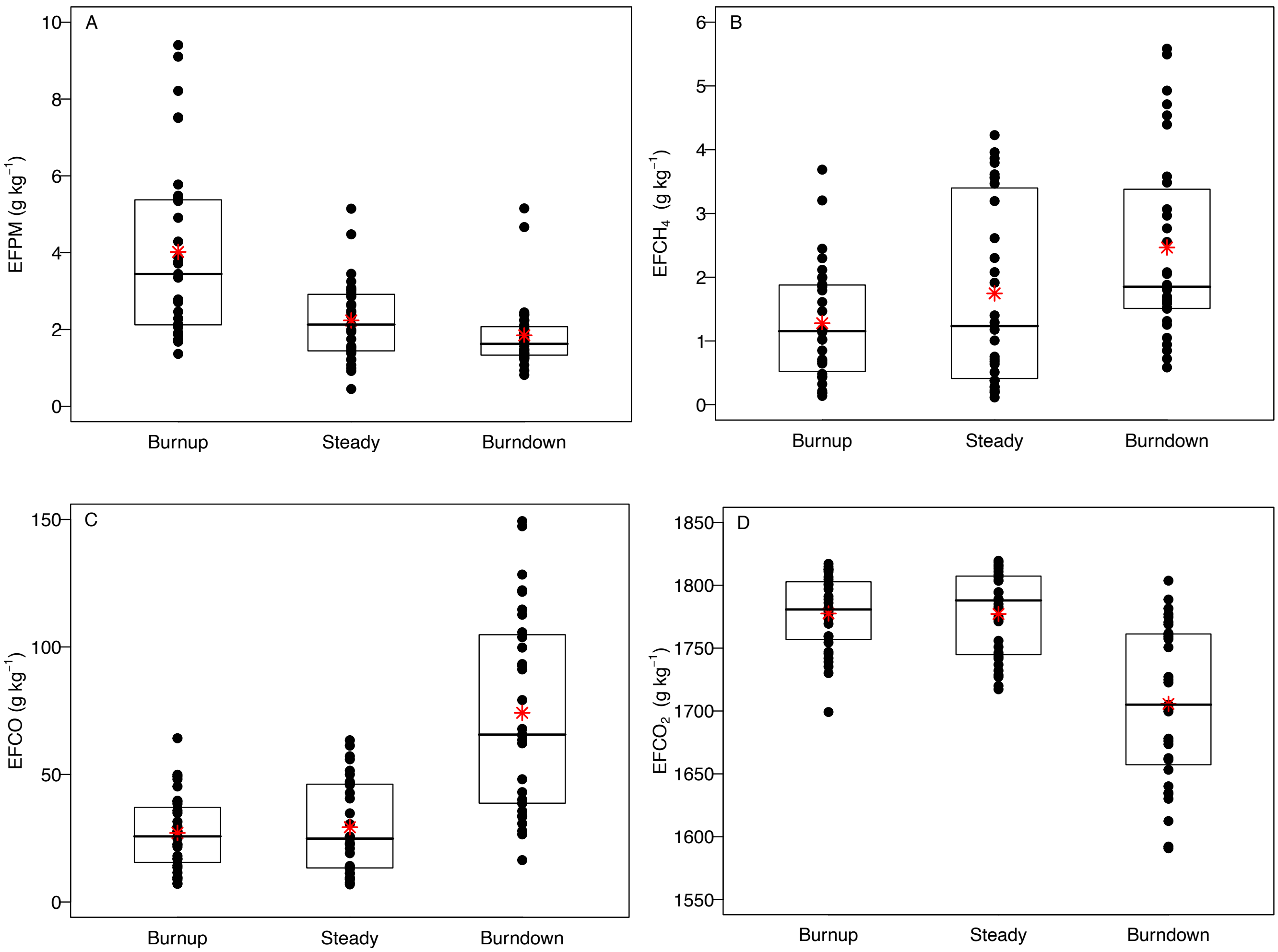

Figure 10—Measured EF (g kg^{-1}) by fire phase. Median (thick black line), lower and upper quartiles (box), mean (red star), and individual values (circles). (A) EFPM, (B) EFCO, (C) $EFCH_4$, and (D) $EFCO_2$. There were 31 measurements per fire phase.

Table 3—The EFs and the MCE summarized by burn phase. The EFs are in units of g kg^{-1} and the MCE is in percent. Values in parenthesis following the means are the standard deviation and the values in parenthesis following the medians are first and third quartiles.

EF/MCE	Burnup	Steady	Burndown
EFPM mean (σ)	4.02 (2.31)	2.24 (1.06)	1.85 (0.93)
EFPM median (Q1, Q3)	3.44 (2.12, 5.38)	2.13 (1.44, 2.92)	1.63 (1.33, 2.07)
$EFCH_4$ mean (σ)	1.28 (0.91)	1.75 (1.45)	2.47 (1.48)
$EFCH_4$ median (Q1, Q3)	1.15 (0.52, 1.88)	1.23 (0.41, 3.40)	1.85 (1.51, 3.38)
EFCO mean (σ)	27.1 (14.7)	29.3 (18.2)	74.2 (38.9)
EFCO median (Q1, Q3)	25.7 (15.5, 37.1)	24.9 (13.4, 46.2)	65.6 (38.7, 104.8)
$EFCO_2$ mean (σ)	1778 (30)	1777 (34)	1706 (63)
$EFCO_2$ median (Q1, Q3)	1781 (1757, 1803)	1788 (1745, 1807)	1705 (1657, 1761)
MCE mean (σ)	97.7 (1.3)	97.5 (1.6)	93.6 (3.4)
MCE median (Q1, Q3)	97.8 (96.8, 98.7)	97.9 (96.0, 98.9)	94.3 (91.0, 96.7)

Figure 11 shows the measured EFs grouped by fire pit type. The data plotted in figure 11 cover all MC, and there is significant burn-to-burn variability. Possible differences in fire pit types are explored with the GLMMs and discussed section 3.1.2.

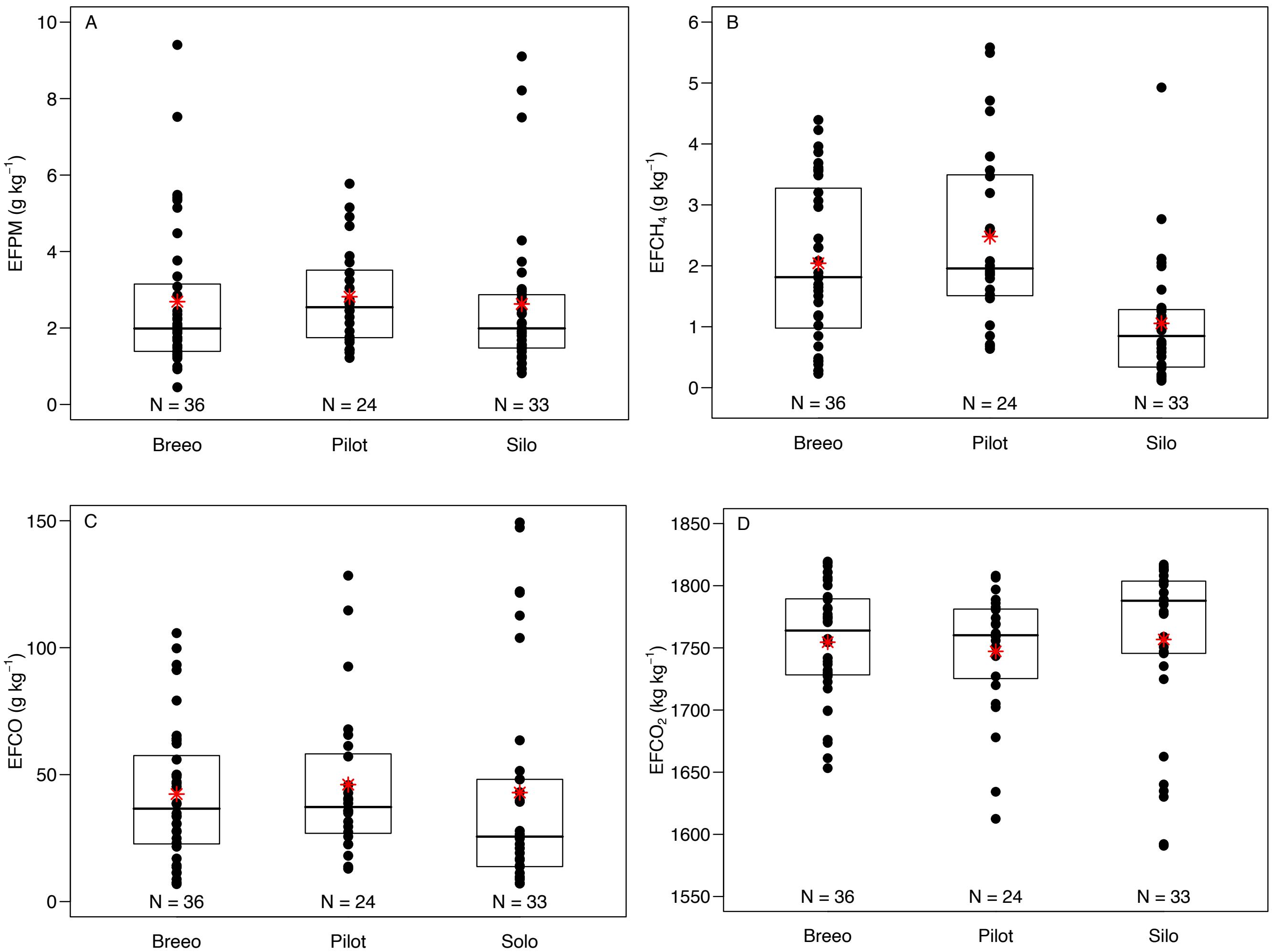

Figure 11—Measured EF ($g\ kg^{-1}$) by fire pit type. Median (thick black line), lower and upper quartiles (box), mean (red star), and individual values (circles). (A) EFPM, (B) EFCO, (C) $EFCH_4$, and (D) $EFCO_2$. N indicates the number of measurements for each fire pit.

3.1.1 Average low-smoke fire pit—

In the open burning of dead forest vegetation (twigs, branches, logs, litter, dead grass), increasing MC tends to reduce CC and $EFCO_2$ and increase EFs for incomplete combustion products such as PM, CH_4, and CO (Urbanski et al. 2022). It was anticipated that MC would have a similar effect on EFs and CC for the burning of firewood in the fire pits. The primary goal of this study is to provide parameters (EFs and CC) for estimating pollutant emissions for the average low-smoke fire pit burning firewood with MC of 10 percent to 30 percent. These parameters are estimated by the GLMMs' MC main effects (section 2.8). The GLMMs' predictions of EFs versus MC were averaged across the three fire pit types (MC main effects) and are shown in figures 12–15. Predicted EF, with 95 percent confidence intervals, for a range of MC are provided in tables 4–7. The GLMMs' estimates of EF response to MC when controlling for fire pit type main effects and MC–fire pit type interactions are given in table 8.

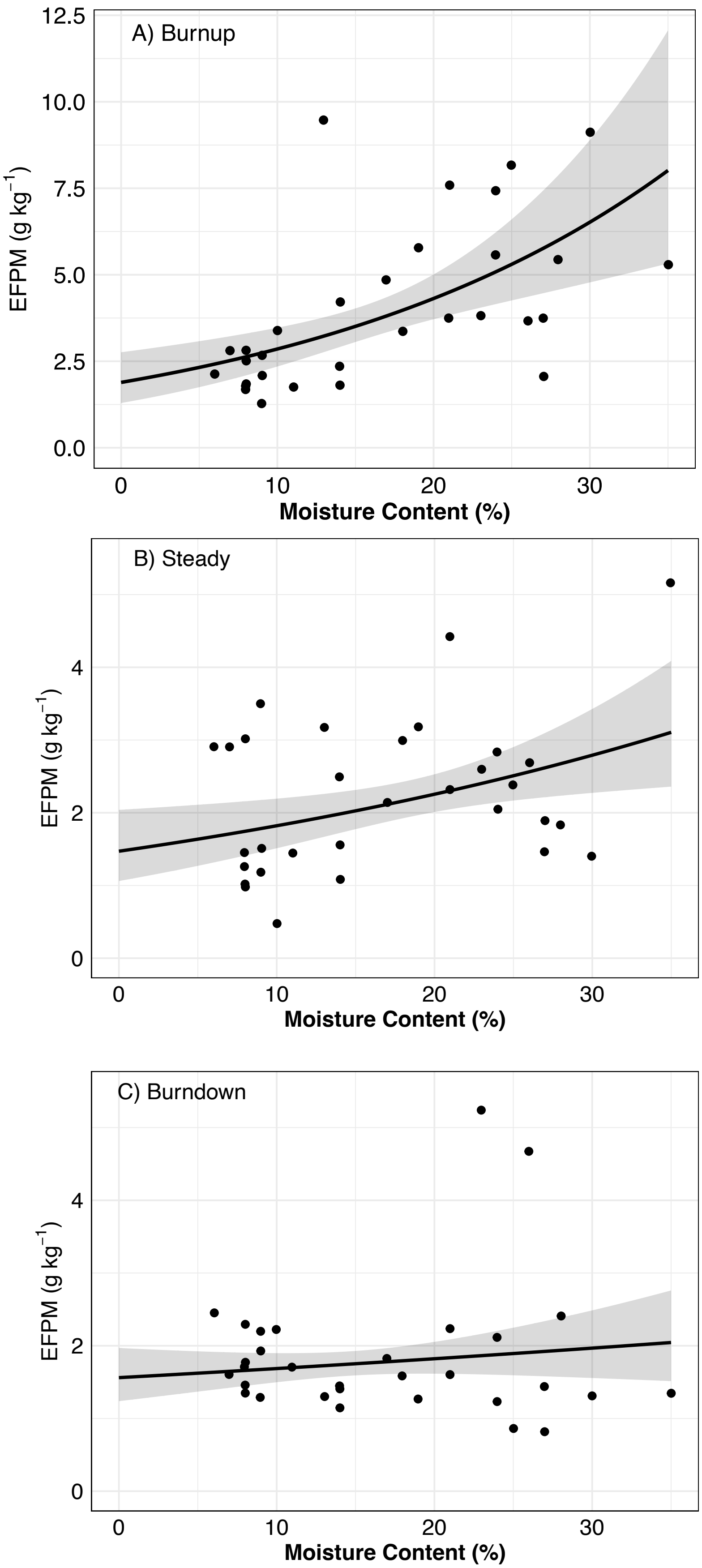

Figure 12—Model estimated EFPM (g kg^{-1}) for the average fire pit (i.e., MC main effect) (solid line) with 95 percent confidence intervals (gray shading). Filled circles are observed EFPM. (A) Burnup phase model, (B) steady phase model, and (C) burndown phase model.

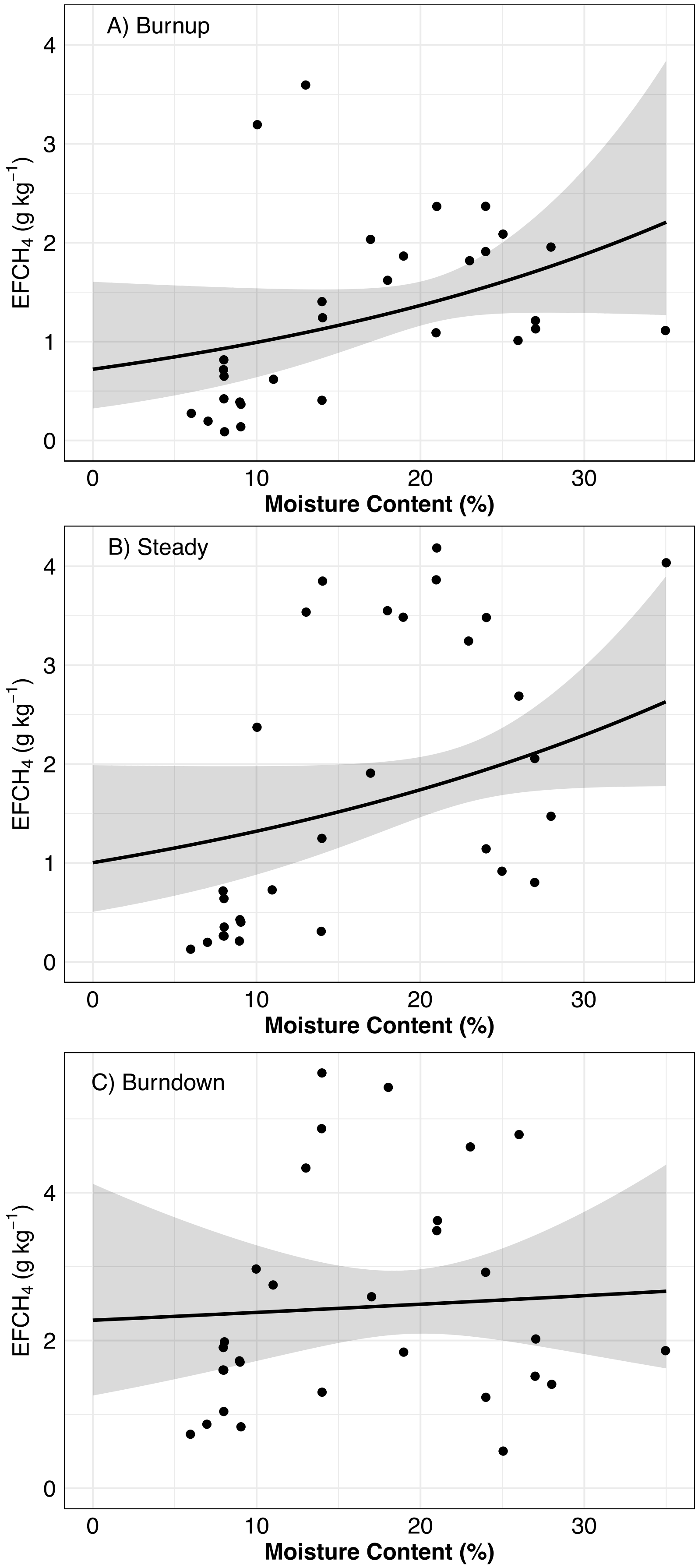

Figure 13—Model estimated $EFCH_4$ ($g\ kg^{-1}$) for the average fire pit (i.e., MC main effect) (solid line) with 95% confidence intervals (gray shading). Filled circles are observed $EFCH_4$. (A) Burnup phase model, (B) steady phase mode, and (C) burndown phase model.

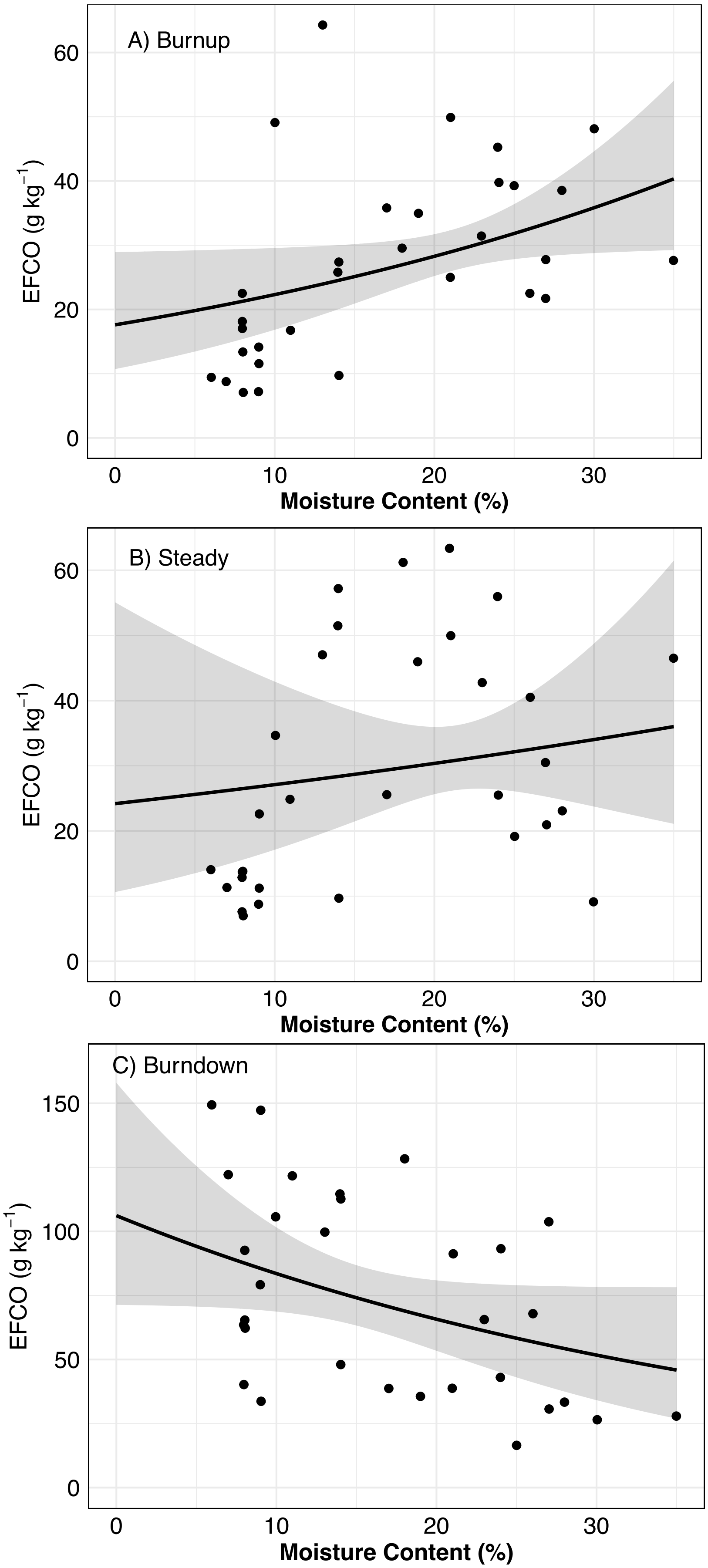

Figure 14—Model estimated EFCO (g kg^{-1}) for the average fire pit (i.e., MC main effect) (solid line) with 95% confidence intervals (gray shading). Filled circles are observed EFCO. (A) Burnup phase model, (B) steady phase model, and (C) burndown phase model.

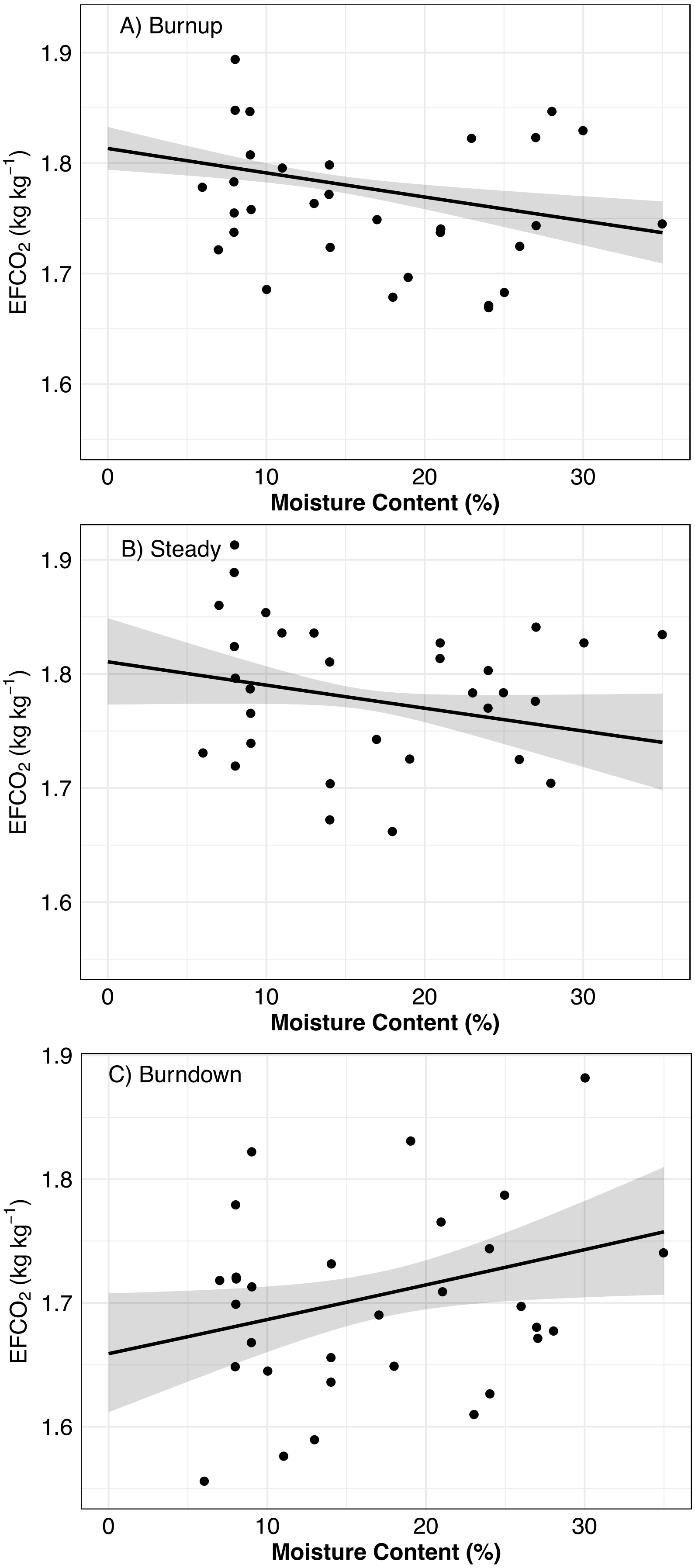

Figure 15—Model estimated $EFCO_2$ (kg kg^{-1}) for the average fire pit (i.e., MC main effect) (solid line) with 95% confidence intervals (gray shading). Filled circles are observed $EFCO_2$. (A) Burnup phase model, (B) steady phase model, and (C) burndown phase model.

Table 4—Model estimated EFPM (g kg^{-1}) for the average low-smoke fire pit as function of MC. The EFPM trend with respect to MC was not significant for the burndown phase model (table 8).

Phase	MC	Predicted EF	Std error[a]	Lower[b]	Upper[b]
Burnup	10	2.85	0.100	2.35	3.47
Burnup	15	3.51	0.070	3.06	4.03
Burnup	20	4.31	0.076	3.71	5.01
Burnup	25	5.30	0.112	4.26	6.61
Burnup	30	6.52	0.159	4.78	8.89
Steady	10	1.82	0.095	1.51	2.19
Steady	15	2.03	0.068	1.77	2.31
Steady	20	2.25	0.059	2.01	2.53
Steady	25	2.51	0.075	2.17	2.90
Steady	30	2.79	0.105	2.27	3.43
Burndown	10	1.69	0.060	1.50	1.90
Burndown	15	1.75	0.049	1.59	1.93
Burndown	20	1.82	0.061	1.62	2.05
Burndown	25	1.89	0.088	1.59	2.25
Burndown	30	1.97	0.120	1.56	2.49

a Standard error

b Upper and lower 95 percent confidence intervals.

Table 5—Model estimated $EFCH_4$ (g kg^{-1}) for the average low-smoke fire pit as a function of the MC. The $EFCH_4$ trend with respect to the MC was not significant for the burndown phase model (see table 8).

Phase	MC	Predicted EF	Std error[a]	Lower[b]	Upper[b]
Burnup	10	0.992	0.224	0.640	1.54
Burnup	15	1.164	0.139	0.887	1.53
Burnup	20	1.366	0.083	1.161	1.61
Burnup	25	1.603	0.113	1.284	2.00
Burnup	30	1.881	0.193	1.289	2.75
Steady	10	1.32	0.206	0.882	1.98
Steady	15	1.52	0.140	1.152	2.00
Steady	20	1.74	0.089	1.461	2.07
Steady	25	2.00	0.086	1.686	2.37
Steady	30	2.29	0.135	1.760	2.98
Burndown	10	2.38	0.165	1.72	3.29
Burndown	15	2.44	0.109	1.97	3.01
Burndown	20	2.49	0.089	2.09	2.96
Burndown	25	2.55	0.124	2.00	3.25
Burndown	30	2.61	0.185	1.82	3.74

a Standard error

b Upper and lower 95 percent confidence intervals.

Table 6—Model estimated EFCO (g kg^{-1}) for the average low-smoke fire pit as a function of the MC. The EFCO trend with respect to the MC was not significant for the burndown phase model (see table 8).

Phase	MC	Predicted EF	Std error[a]	Lower[b]	Upper[b]
Burnup	10	22.3	0.144	16.8	29.6
Burnup	15	25.1	0.094	20.9	30.2
Burnup	20	28.3	0.059	25.2	31.7
Burnup	25	31.8	0.068	27.8	36.4
Burnup	30	35.8	0.112	28.8	44.6
Steady	10	27.1	0.235	17.1	42.9
Steady	15	28.7	0.148	21.4	38.4
Steady	20	30.4	0.086	25.6	36.0
Steady	25	32.1	0.107	26.1	39.6
Steady	30	34.0	0.184	23.7	48.8
Burndown	10	83.5	0.100	68.7	101.6
Burndown	15	74.1	0.081	63.2	86.8
Burndown	20	65.7	0.106	53.4	80.9
Burndown	25	58.3	0.155	43.0	79.0
Burndown	30	51.7	0.212	34.1	78.4

a Standard error

b Upper and lower 95% confidence intervals.

Table 7—Model estimated $EFCO_2$ (kg kg^{-1}) for the average low-smoke fire pit as function of the MC. The $EFCO_2$ trend with respect to the MC was not significant for the burndown phase model (see table 8).

Phase	MC	Predicted EF	Std error[a]	Lower[b]	Upper[b]
Burnup	10	1.79	0.002	1.78	1.80
Burnup	15	1.78	0.002	1.77	1.79
Burnup	20	1.77	0.003	1.76	1.78
Burnup	25	1.76	0.005	1.74	1.77
Burnup	30	1.75	0.006	1.73	1.77
Steady	10	1.79	0.005	1.77	1.81
Steady	15	1.78	0.003	1.77	1.79
Steady	20	1.77	0.004	1.76	1.78
Steady	25	1.76	0.006	1.74	1.78
Steady	30	1.75	0.009	1.72	1.78
Burndown	10	1.69	0.008	1.66	1.71
Burndown	15	1.70	0.006	1.68	1.72
Burndown	20	1.72	0.006	1.70	1.74
Burndown	25	1.73	0.008	1.70	1.76
Burndown	30	1.74	0.011	1.70	1.78

a Standard error

b Upper and lower 95 percent confidence intervals.

Table 8—GLMMs' Moisture Content Main Effects

Emission Species	Phase	MC[a]	MC trend[b]	SE[c]	LCL[d]	UCL[d]	z-ratio[e]	p-value[f]
EFPM	Burnup	16.8	0.041	0.011	0.02	0.063	3.82	<0.001
EFPM	Steady	16.8	0.021	0.008	0.005	0.037	2.63	0.008
EFPM	Burndown	16.8	0.008	0.007	-0.006	0.022	1.06	0.287
$EFCH_4$	Burnup	16.4	0.032	0.019	-0.006	0.07	1.67	0.095
$EFCH_4$	Steady	16.4	0.028	0.015	-0.002	0.057	1.84	0.066
$EFCH_4$	Burndown	16.4	0.005	0.015	-0.025	0.034	0.301	0.763
EFCO	Burnup	16.8	0.024	0.011	0.001	0.046	2.07	0.039
EFCO	Steady	16.8	0.011	0.019	-0.026	0.049	0.592	0.554
EFCO	Burndown	16.8	-0.024	0.013	-0.049	0.001	-1.88	0.060
$EFCO_2$	Burnup	16.8	-0.001	0	-0.002	0	-3.3	0.001
$EFCO_2$	Steady	16.8	-0.001	0.001	-0.002	0	-1.77	0.077
$EFCO_2$	Burndown	16.8	0.002	0.001	0	0.003	2.09	0.037

a Study mean MC (%)

b Response of EF to MC on log scale

c Standard error of MC trend

d Lower and upper 95% confidence intervals for MC trend.

e Wald statistic

f p-value calculated from the Wald statistic

The modeled EFPM response to MC is positive (EFPM increases with increasing MC) for all burn phases (fig. 12) but is only statistically significant for the burnup and steady phases (table 8). The EFPM response to MC is stronger during the burnup phase than the steady phase (table 8), e.g. increasing MC from 15 percent to 25 percent increases the burnup phase EFPM by 51 percent (1.79 g kg^{-1}), compared with 24 percent (0.48 g kg^{-1}) for the steady phase (table 4). Across the MC range tested, predicted EFPM consistently decreases across phases from burnup to steady to burndown (table 4). At the benchmark MC of 20 percent, the burnup phase EFPM is roughly twice that of the steady phase.

As with EFPM, $EFCH_4$ tended to increase with MC in the burnup and steady phases and the modeled $EFCH_4$ response to MC is positive (fig. 13). However, unlike EFPM, the magnitude of the $EFCH_4$ response to MC is similar for the burnup and steady phases, and the model statistics indicate the relationship is less robust (not significant at the p = 0.05 level) (table 8). Across burn phases, modeled $EFCH_4$ follow the trend burnup < steady < burndown (table 5), which is the opposite of that for EFPM. At MC = 20 percent, $EFCH_4$ of the burndown phase (2.49 g kg^{-1}) is about 80 percent higher than the burnup phase (1.37 g kg^{-1}).

The modeled EFCO for burnup and steady burn phases agrees within 20 percent across the MC range of the tests, while the burndown phase is substantially larger than either the burnup or steady phases (table 6). At MC = 20 percent burndown phase, EFCO is about twice that of the burnup and steady burn phases. The burnup and burndown phase EFCO response to MC is similar in magnitude, but in the reverse direction (fig. 14, table 8). The steady phase response to MC is not significant (p-value=0.55, table 8). There is a minimal difference in model-predicted $EFCO_2$ among burn phases or across MC (table 7). The models predicted the same $EFCO_2$ for the burnup and steady phase for a given MC, and the burndown phase $EFCO_2$ is just a few percent lower.

We anticipated MC to have a noticeable effect on EF during the burnup phase when firewood is added at short intervals. Indeed, the models indicate that EFPM, $EFCH_4$, and EFCO increase, and $EFCO_2$ decreases with increasing MC during the burnup phase (table 8). This behavior persists into the steady phase except for EFCO, for which the response is not significant (p-value=0.55). In the steady phase, the $EFPM_{2.5}$ response to MC is roughly half that of the burnup phase. In contrast, the magnitude of the $EFCH_4$ and EFCO responses to MC differ only slightly between the burnup and steady phases.

The burndown phase was characterized by glowing combustion of charred wood (fig. 4). For fixed MC, the burndown phase has the lowest EFPM and EFCO2 and highest EFCO and $EFCH_4$. Since the burndown phase is defined as starting 10 minutes after the last firewood addition of the steady phase, it is likely much of the water would have evaporated and we would not expect an MC effect to be observed for this phase. This is the case for $EFCH_4$ and EFPM. However, the model indicates a notable response for EFCO (negative) and $EFCO_2$ (positive) to MC. It is unclear by what mechanism MC would affect burndown phase EFCO and $EFCO_2$.

3.1.2 Fire pit type main effects and fire pit type–MC interactions—

This section provides information on EFs differences among the three fire pit types tested. The GLMMs' fire pit type main effects identify differences in EFs at the study mean MC (16.3%), while the GLMMs' fire pit type–MC interactions identify differences in the response of the fire pits to MC. Model results for fire pit type main effects and fire pit type–MC interactions are provided for EFPM, $EFCH_4$, EFCO, and $EFCO_2$ in Appendices C, D, E, and F, respectively.

There is no evidence of a fire pit type main effect for EFPM during the burnup or steady phases (Appendix C, table C.2). However, during the burndown phase, at study average MC, EFPM order as Solo < Breeo < Pilot, with the difference between the Solo (1.43 g kg^{-1}) and Pilot (2.28 g kg^{-1}) being statistically strong (p-value < 0.002) (Appendix C, table C.2). For the burnup phase, the Solo $EFCH_4$ at the study average MC (0.72 g kg^{-1}) is significantly lower than that for either the Breeo (1.72 g kg^{-1}) or Pilot (1.45 g kg^{-1}) (Appendix D, tables D.1 and D.2). Similarly, for the steady phase, the Solo $EFCH_4$ at the study average MC (0.69 g kg^{-1}) is significantly lower than that for either the Breeo (2.16 g kg^{-1}) or Pilot (2.62 g kg^{-1}) (Appendix D, tables D.1 and D.2). In the burnup phase, the EFCO at the study average MC for the Solo (19.4 g kg^{-1}) is significantly lower than that for the Breeo (32.9 g kg^{-1}) and Pilot (28.2 g kg^{-1}) (Appendix E, tables E.1 and E.2).

Interestingly, the burnup and steady phase EFPM models indicate a negative MC response for the Solo, contrary to the trend for Breeo and Pilot (Appendix C, tables C.3 and C.4) and the average low-smoke fire pit (section 3.1.1; table 8). During the burnup phase, the Solo $EFCH_4$ has a positive response to MC that is significantly stronger than the Breeo and Pilot (Appendix D, tables D.3 and D.4). As with the $EFCH_4$, during the burnup phase, the Solo EFCO has a positive response to MC that is stronger than the Breeo and Pilot (Appendix E, tables E.3 and E.4). The $EFCO_2$ models indicate that fire pit type main effects and fire pit type–MC interactions are negligible (Appendix F, tables F.1-F.4).

In summary, during the steady phase, the Solo fire pit EFPM had a negative response to MC, and EFPM increased with decreasing MC, contrary to expectations. The Solo $EFCH_4$ at the study average MC was about ½ to ⅓ that of the Breeo and Pilot during the burnup and steady phase, respectively. For the burnup phase, the Solo $EFCH_4$ and EFCO positive responses to MC were much stronger than that of the Breeo or Pilot.

3.2 Particle Size

Atmospheric particulate matter is often described according to size. Particle size is generally classified using aerodynamic diameter thresholds; for example, $PM_{2.5}$ is defined as particles with a nominal aerodynamic diameter ≤2.5 µm. In this study, the focus has been on $PM_{2.5}$ due to its detrimental impacts on health and visibility and its designation as a criteria pollutant under the Federal Clean Air Act (USEPA 2021, 2019). The particles in fresh smoke resulting from the burning of wildland fuels—dead forest and rangeland biomass (needles, leaves, cones, grass, twigs, branches, logs, and peat)—are predominantly PM_1 (particles of diameter ≤1 µm) (Hosseini et al. 2010; Reid et al.

2005). During round 3 of fire pit testing, particle size distributions were measured for three burns. These measurements of particle size may be useful in understanding the potential air quality and health impacts of the smoke produced by recreational fire pits.

Visiting researchers from the University of Wyoming measured particle size distributions (section 2.6.1) for three burns: BurnID 2021061004, 2021061105 and 2021061506 (table 1). Table 9 lists the mass median particle diameters (MMD; the diameter for which smaller particles comprise half the total particle mass) by phase for these three burns. The particle MMD were consistently well below 1 µm, as expected (Hosseini et al. 2010; Reid et al. 2005). Figure 16 plots Signal-to-Noise ratio (SNR) for particle number counts by particle size bin for the three burns listed in table 9. The SNR for each size bin was determined from a ratio of the mean and standard deviation of raw electrometer measurements (current signal) for each impactor stage during a steady 100 s period of particle collection. The particle count drops dramatically for sizes greater than 1 µm and SNR plummets, indicating the minimal presence of larger particles. The measurement results shown in figure 16 and table 9 confirm that particle mass was minimal for particle diameter >1µm.

Table 9—Mass median diameter measured for different phases of three burns. Values in parentheses are one standard deviation.

BurnID	Firepit	Burn phase	Mass median diameter (µm)
2021061004	Solo	Burnup	0.130(0.028)
2021061004	Solo	Steady	0.261(0.042)
2021061004	Solo	Burndown	0.246(0.073)
2021061105	Solo	Burnup	0.190(0.064)
2021061105	Solo	Steady	0.254(0.068)
2021061105	Solo	Burndown	0.241(0.144)
2021061506	Breeo	Burnup	0.182(0.116)
2021061506	Breeo	Steady	0.189(0.031)
2021061506	Breeo	Burndown	0.227(0.077)

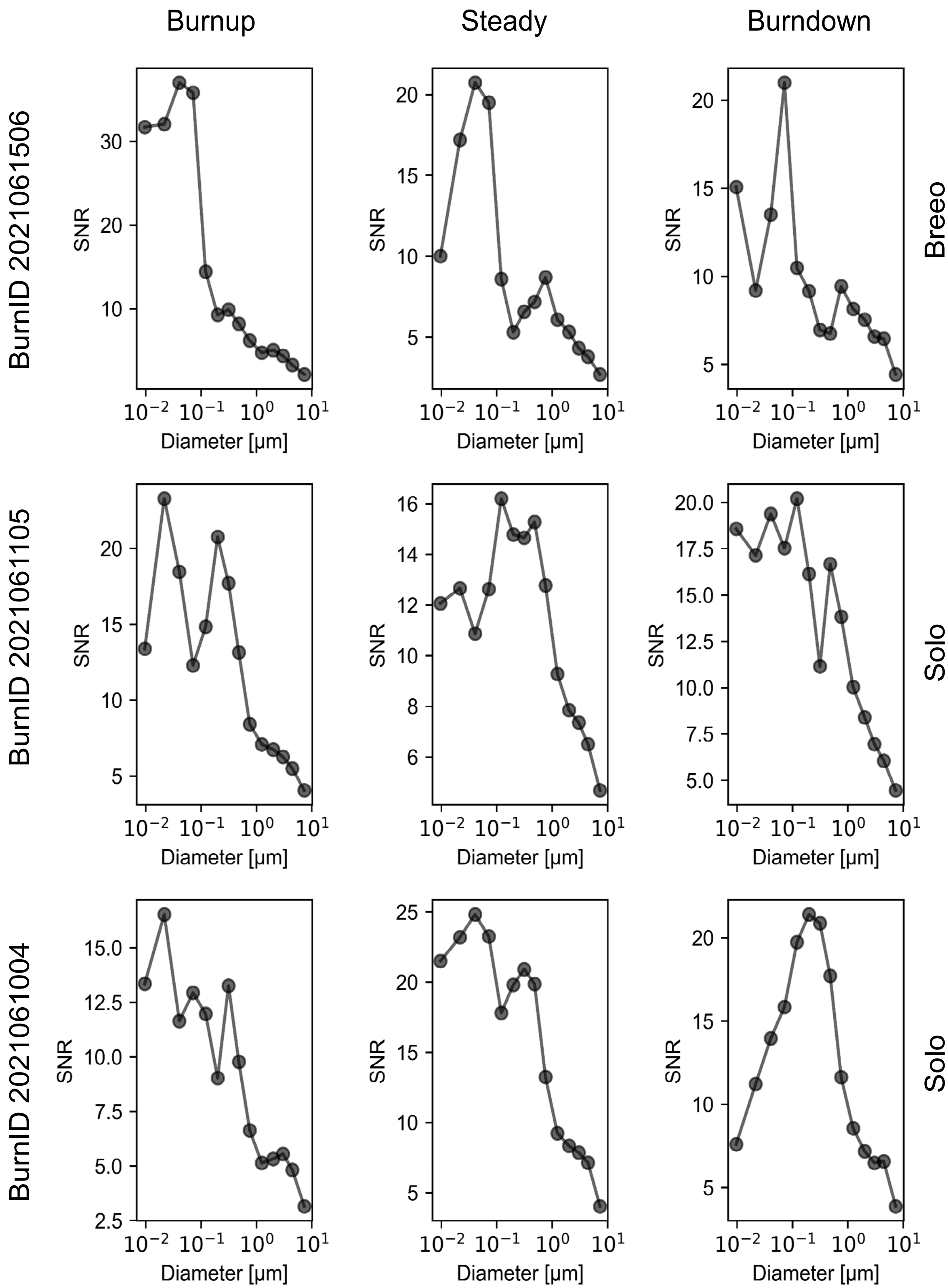

Figure 16—Signal-to-Noise ratio (SNR) for particle number counts by particle size bin from a representative fire pit test during round 3. The particle count drops dramatically for sizes greater than 1 μm and SNR plummets. The SNR for each size bin was specifically determined from a ratio of the mean and standard deviation of raw electrometer measurements for each impactor stage during a steady 100-second period of aerosol collection.

3.3 Comparison with Previous Results

The purpose of this project was to determine if self-advertised low-smoke fire pits produce less $PM_{2.5}$ than traditional fire pits, and if so, evaluate the potential of reducing PM pollution by replacing traditional fire pits with the low-smoke variety. In this section we compare EFs measured in our study with those used in the USEPA National Emission Inventory (NEI), a triennial, comprehensive estimate of air pollutant emissions for the U.S. (USEPA 2023b). In the NEI, outdoor residential recreational fire pit use is categorized as "residential wood combustion" (RWC), in the subcategory of "outdoor wood burning device" (Source Classification Code (SCC) 2104008700). The NEI EFs for the residential wood combustion sector and other SCCs whose default emissions are estimated by the USEPA are compiled in the Wagon Wheel for Nonpoint Sources (USEPA 2023b). Table 10 compares steady phase EFPM and EFCO from our study for MC = 20 percent with those for the NEI (EFPM_NEI and EFCO_NEI). The EFPM_NEI and EFCO_NEI are EFs for fireplaces burning cordwood (USEPA 2023b; Houck and Eagle 2006; Houck et al. 2001) and are used as a proxy for outdoor recreational burning in both traditional and low-smoke fire pits as well as other devices. Included in table 10 are EFs from the literature for pile burning—the open burning of piled woody debris (slash piles) from the mechanical thinning or cutting of trees in forests. In the large body of EF studies of wildfire and prescribed burning, pile burning is the most analogous to burning of cordwood in recreational fire pits. The pile burn EFs are based on measurements of burning "wet" and "dry" piles measuring 3 m x 3 m and 6.1 m x 6.1 m (Aurell et al. 2017); the authors do not provide an estimate of moisture content associated with the "wet" and "dry" classifications.

Table 10—Comparison of the EFs (g kg^{-1}) measured in this study at MC = 20 percent with EFs for NEI/fireplaces and pile burning. The EFPM, $EFCH_4$, and EFCO for this study are from tables 4, 5, and 6, respectively. The NEI values are based emission measurements for fireplaces. Aurell et al. 2017 apply to the EFs for pile burns.

EF	Steady phase for this study[a]	NEI	Houck and Eagle (2006)[b] (g kg^{-1})	Aurell et al. (2017)[c] wet	Aurell et al. (2017)[c] dry
$PM_{2.5}$	2.25(2.01, 2.53)	11.8(11.6)[b,d,e]	15.3	18	4.5
CO	30.4(25.6,36.0)	74.63	74.6	82	29
CH_4	1.74(1.46,2.07)	—	7.21	5.7	1.1

a Values in parentheses are 95 percent confidence intervals.

b Wagon Wheel (USEPA 2023b).

c The authors do not provide an estimate of moisture content associated with the "wet" and "dry" classifications.

d Value in parentheses is one standard deviation.

e Houck et al. 2001.

The EFPM_NEI is a factor of 5.2 greater than the EFPM we measured for low-smoke fire pits. This difference may be partly attributable to the testing methodology. Likewise, EFCO_NEI and fireplace $EFCH_4$ (Houck and Eagle 2006) are also much larger than those measured in our testing, by factors of 2.4 and 4.1, respectively. Our results show that the low-smoke fires pits tested in our study produce significantly less PM and CO (per mass of firewood consumed) than traditional fire pits or fire rings, assuming that EFPM_NEI and EFCO_NEI reasonably characterize the latter wood burning appliances. Thus, if the use of fire pits like those tested in our study is widespread, the NEI may overestimate PM and CO emissions from residential outdoor recreational wood burning. While CH_4 is not a pollutant tracked in the NEI, it is an atmospheric pollutant of interest. Our testing indicates that low-smoke fire pits have a much lower $EFCH_4$ than cordwood fireplaces (Houck and Eagle 2006). The EFs for wet pile burning (Aurell et al. 2017) are similar to those reported for fireplaces burning cordwood (Houck and Eagle 2006), while the EFs for dry pile burning closely match the steady phase EFs measured in our testing.

3.4 Methods for Calculating Firewood Consumption and Emissions

In addition to determining if low-smoke fire pits produce less PM than traditional fire pits, our study's other objective was to assess the potential for reducing PM emissions by replacing traditional fire pits with the low-smoke variety. In this section we present equations and parameters based on our testing that can be used to estimate PM emissions from outdoor recreational fire pits. In section 4, these equations and parameters are used to model PM emissions from estimates of firewood use. As in preceding sections, firewood mass (input or consumption) is the dry-weight mass (see section 2.3) unless stated otherwise.

Air emissions of pollutant X from open wood burning, such as outdoor recreational fire pits, are commonly calculated as:

$$EX = FC \times EFX \tag{3}$$

where EX is the mass of pollutant X emitted (g), FC is the mass of firewood consumed (kg), and EFX is the emission factor for X (g-X per kg-firewood consumed). We reiterate that firewood consumed refers to the mass of firewood volatilized as gases and particulates and does not include charcoal and ash (section 2.4).

Recreational fire pit use can be modeled with the three distinct phases used in our emission testing: burnup, steady, and burndown. The emission equation expands to account for differences in EFX and FC between phases:

$$EX = FC_{bu}EFX_{bu} + FC_{sb}EFX_{sb} + FC_{bd}EFX_{bd} \tag{4}$$

where the subscripts bu, sb, and bd refer to the phases (burnup, steady, and burndown, respectively). Analysis of the emissions measurements from our testing provided estimates of EFPM, $EFCH_4$, EFCO, and $EFCO_2$ for the average low-smoke fire pit for each burn phase (tables 4–7). Here we focus on estimating FC based on assumptions regarding user behavior—the duration (t) and firewood input (FW) for each fire phase—and CC measured in our testing (section 2.4) and analyzed with GLMMs (section 2.8) to provide burn phase specific estimates of CC for the average fire pit.

3.4.1 Combustion completeness—

The open burning of biomass is influenced by MC with the burning rate and CC of dead wood tending to decrease with increasing MC (Ottmar 2014; Prichard et al. 2022). The dependence of CC on MC for the average low-smoke fire pit is provided by the GLMMs' MC main effects (section 2.8). The GLMMs' predictions of CC *versus* MC averaged across the three fire pit types (MC main effects) are shown in figure 17 and tabulated for MC 10–30 percent in table 11. The GLMMs' estimates of CC response to MC for the average low-smoke fire pit are given in table 12. For all three burn phases, CC decreases with increasing MC as anticipated (fig. 17). The magnitude of the CC response to MC is similar across the three phases (table 12). We emphasize that the burndown phase allowed the fire to burnout and smolder over a 20–30 minute period and was then extinguished. Allowing the burndown phase to continue for longer would result in greater FC and CC. Therefore, our burndown phase model predictions of CC are only applicable to a burndown phase of 20 to 30 minutes.

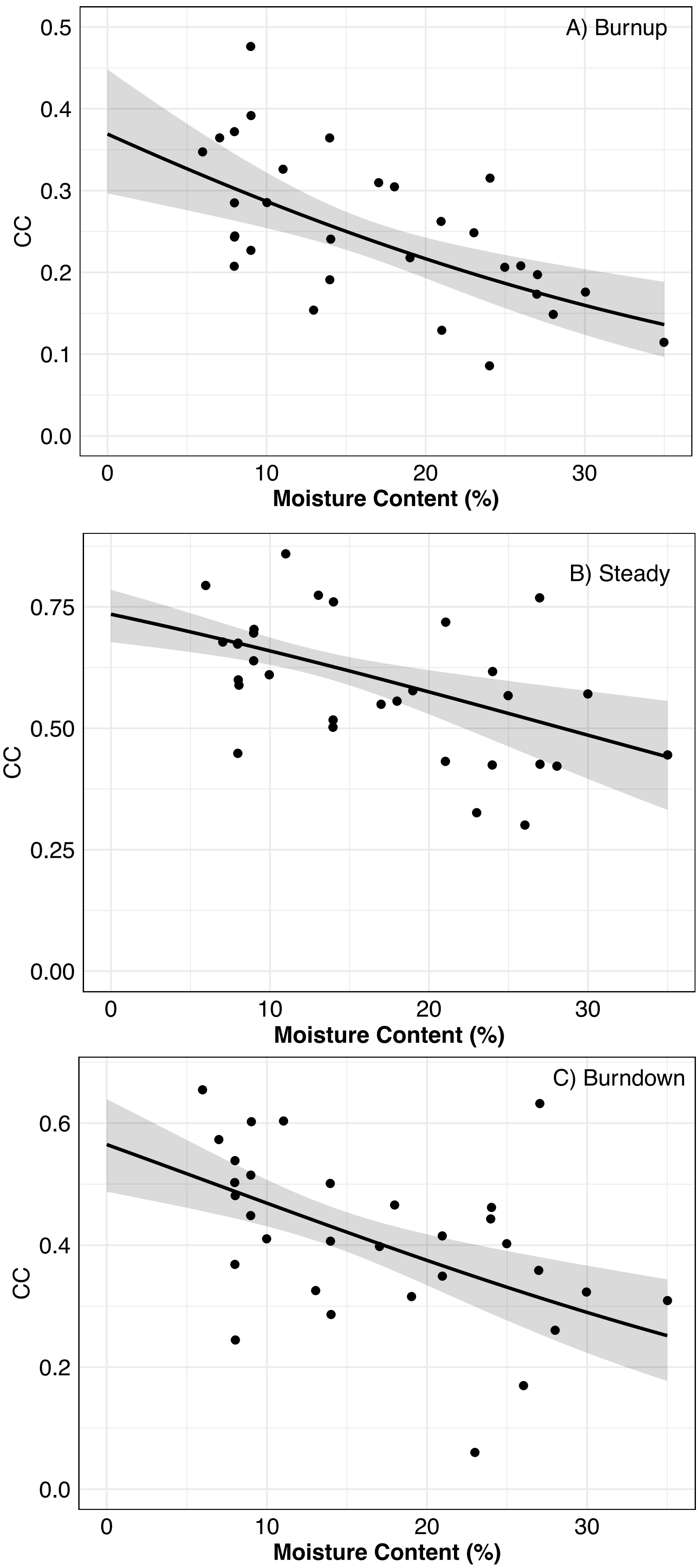

Figure 17—Model estimated CC for the average fire pit (i.e., MC main effect) (solid line) with 95 percent confidence intervals (gray shading). Filled circles are observed CC.

Table 11—Model predicted CC (unitless, range of 0–1) for the average low-smoke fire pit as a function of MC.

Phase	MC	Predicted CC	Std error[a]	Lower[b]	Upper[b]
Burnup	10	0.287	0.085	0.254	0.322
Burnup	15	0.250	0.063	0.227	0.274
Burnup	20	0.217	0.075	0.193	0.243
Burnup	25	0.186	0.110	0.156	0.221
Burnup	30	0.160	0.152	0.124	0.204
Steady	10	0.659	0.064	0.631	0.687
Steady	15	0.618	0.063	0.588	0.647
Steady	20	0.575	0.095	0.529	0.620
Steady	25	0.531	0.139	0.462	0.598
Steady	30	0.486	0.187	0.396	0.577
Burndown	10	0.469	0.078	0.431	0.507
Burndown	15	0.421	0.068	0.389	0.454
Burndown	20	0.375	0.091	0.334	0.418
Burndown	25	0.331	0.132	0.276	0.391
Burndown	30	0.290	0.178	0.223	0.366

a Standard error

b Upper and lower 95 percent confidence intervals.

In section 3.4.4 we described how our test data can be used to estimate CC for an arbitrary burndown period. In contrast, the burnup and steady phases involved the initiation and maintenance of a steady fire through continuous, regular additions of firewood. Therefore, model predicted CC for these phases are applicable to longer durations than those used in testing if the cadence of firewood addition is similar with that used in our testing (section 2.4). The GLMMs indicate fire pit type main effects and fire pit type-MC interactions are negligible for CC (Appendix G, tables G.1-G.4), that is, burn phase and MC are more important in determining CC than fire pit type.

3.4.2 Burnup phase—

In our testing, the burnup phase was designed to initiate a robust, steady fire (see section 2.4). Burnup phase PM emissions (E_{bu}) can be estimated using equation 5:

$$E_{bu} = EF_{bu} FW_{bu} \frac{CC_{bu}}{100} \tag{5}$$

where FW_{bu} is the firewood input during the burnup phase, CC_{bu} is burnup phase combustion completeness and EF_{bu} is the PM emission factor for the burnup phase. The burnup phase firewood input rate (FWR_{bu}; g s^{-1}) over the 31 tests is summarized in Appendix H, figure H.1; median FWR_{bu} = 10.3 g s^{-1} (0.62 kg $minute^{-1}$). Since this fuel input rate successfully initiated a vigorous fire in our tests and followed operation instructions of the Solo and Breeo manufacturers, we combine this value with an assumed burnup phase duration of t_{bu} = 20 minutes (close to our study median of 22.5 minutes) to derive a default estimate of FW_{bu} = 12.4 kg. This value for FW_{bu} can be employed in equation 5 with burnup phase values for EFPM (table 4) and CC (table 12) at the MC of interest to calculate E_{bu}.

Table 12—GLMMs' moisture content main effects for CC models.

Phase	MC[a]	MC trend[b]	SE[c]	LCL[d]	UCL[d]	z-ratio[e]	p-value6[f]
Burnup	16.8	-0.037	0.01	-0.057	-0.018	-3.83	< 5.00E-04
Steady	16.8	-0.036	0.01	-0.056	-0.016	-3.51	< 5.00E-04
Burndown	16.8	-0.039	0.01	-0.059	-0.018	-3.75	< 5.00E-04

a Study mean MC (percent)

b Response of CC to MC on log scale

c Standard error of MC trend

d Lower and upper 95 percent confidence intervals for MC trend.

e Wald statistic

f p-value calculated from the Wald statistic

3.4.3 Steady phase—

The steady phase represents fire pit operation that is expected to be responsible for the majority of firewood burned in fire pits. During the steady phase, firewood was added at a semi-regular interval of approximately 10 minutes over a period of 45–60 minutes. PM emissions for the steady phase (E_{sb}) can be estimated using equation 6:

$$E_{sb} = EF_{sb}\frac{CC_{sb}}{100}(FW_{sb} + FW_{bux}) \tag{6}$$

where EF_{sb}, CC_{sb}, and FW_{sb} are the PM emission factor, combustion completeness, and firewood added for the steady phase, respectively. The FW_{bux} is firewood remaining from the burnup phase:

$$FW_{bux} = \left(1 - \frac{CC_{bu}}{100}\right)(FW_{bu}) \tag{7}$$

The steady phase firewood input rate (FWR_{sb}; g s^{-1}), which does not include the firewood remaining from the burnup phase, is summarized in Appendix H, figure H.1 for the 31 tests. The median FWR_{sb} was 3.1 g s^{-1} (0.19 kg $minute^{-1}$). The burnup phase initiated a robust fire, and a substantial amount of unburnt firewood carried over to the steady phase. This is likely one of the reasons a comparatively low firewood input rate (3.1 g s^{-1} *versus* 10.3 g s^{-1}) was sufficient to maintain a vigorous and stable fire during the steady phase. Given the steady phase duration (t_{sb}) FW_{sb} can be calculated from FWR_{sb} and then equation 6 can be used to calculate E_{sb} using the FW_{bux} and steady phase values for EFPM (table 4) and CC (table 12) at the MC of interest.

3.4.4 Burndown phase—

The burndown phase simulates postfire smoldering and is taken to begin about 10 minutes after the final firewood addition of steady phase. Users could extinguish the smoldering fire or allow it to smolder to extinction. Our tests monitored the burndown phase for 20 to 30 minutes to measure EFs and firewood consumption rate (FCR). The PM emissions for the burndown phase (E_{bd}) can be estimated using equation 8:

$$E_{bd} = EF_{bd}FC_{bd} \tag{8}$$

where EF_{bd} is the burndown EF_{PM} at a given MC (table 4) and FC_{bd} is the firewood consumed. The FC_{bd} depends on the amount of firewood remaining from the steady phase (FW_{sbx}) and the duration (t_{bd}) and fuel consumption rate (FCR_{bd}) of the burndown phase:

$$FC_{bd} = \min\{FCR_{bd}t_{bd}, 0.90FW_{sbx}\} \tag{9}$$

where

$$FW_{sbx} = \left(1 - \frac{CC_{sb}}{100}\right)(FW_{sb} + FW_{bux}) \tag{10}$$

Equation 9 allows one to consider a variable burndown time (t_{td}), for example, allowing the fire to smoldering for 60 minutes and then extinguishing or allowing the fire to smolder to extinction. If the fire pit is allowed to smolder to extinction it is assumed that 10 percent of the firewood mass carried over from the steady phase is left as ash and char ($0.90FW_{sbx}$ in equation 9). Appendix H, figure H.1 summarizes FCR_{bd}, which had a median value of 2.3 g s^{-1}.

4. Emission Inventory

4.1 Model Burn

In section 3.4 we presented equations for calculating phase specific quantities, such as E_{sb}, CC_{sb}, and FC_{sb}, from our measurements of gas and particulate emissions and burn integrated FC. In this section we demonstrate a method for using the equations in section 3.4 with our project's fire pit testing data to calculate a PM emission inventory for outdoor recreational wood burning with low-smoke fire pits. The methodology assumes emissions are calculated from an inventory of firewood use, that is the amount of firewood consumed (FC) during a fire is not known and must be calculated. Additionally, the methodology requires assumptions regarding user behavior, in particular: (1) the duration of the burnup and steady burning phases, and (2) whether the fire is extinguished or allowed to smolder to extinction.

We begin by constructing a baseline model recreational burn to represent the average fire by a typical user. The baseline model burn assumes a fire pit that performs like those tested in our study, that is fueled with split hardwood. The model burn assumes a 20-minute burnup phase and 120-minute steady phase with firewood use rates based on the values from the testing (table 13). The model burn assumes the fire pit users allow the fire to smolder to extinction during the burndown phase with 90 percent of the firewood present at the beginning of the burndown phase ($0.90FW_{sbx}$, equation 10) being consumed. Given firewood MC, burn phase specific EFPM (table 4) and CC (table 11) values can be combined with burn phase durations and firewood input rates (table 13) to calculate E_{bu}, E_{sb}, and E_{bd} using equations 5–10. Summing E_{bu}, E_{sb}, and E_{bd} allows for the calculation of a burn average EFPM based on firewood input ($EFPM_{burn}$; g PM per kg firewood input):

$$E_{burn} = EFPM_{burn} FW_{burn} = E_{bu} + E_{sb} + E_{bd} \qquad (11)$$

Table 13—Parameter values for model recreational burn.

Parameter	Value	Description
t_{bu}	20 minute	Duration of burnup phase from fire pit tests
t_{sb}	120 minute	Duration of steady phase, estimate for a typical recreational burn
FWR_{bu}	0.62 kg minute^{-1}	Burnup phase firewood input rate from fire pit tests (Appendix H). Firewood dry weight mass.[a]
FWR_{sb}	0.19 kg minute^{-1}	Steady phase firewood input rate from fire pit tests (appendix H). Firewood dry weight mass.[a]
FCR_{bd}	0.14 kg minute^{-1}	In the baseline recreational burn the fire is allowed to smolder to extinction which is assumed to occur when 90 percent of firewood present at start of burndown phase (Eq. 10) has burned.

a Firewood wet mass, M_{wet}, may be calculated as $M_{wet} = M_{dry}*((MC/100) + 1)$, where M_{dry} is the firewood dry-weight mass and MC is firewood moisture content as percent of dry mass (see section 2.3).

This model recreational burn uses 35.2 kg of firewood (FW_{burn}) which is calculated from the parameters in table 13: $FW_{burn} = t_{bu}FWR_{bu} + t_{sb}FWR_{sb}$. Assuming firewood MC = 20 percent, the commonly recommended upper limit for good wood-burning practices (see e.g., https://www.epa.gov/burnwise), phase specific PM emissions were then calculated using equations 5–10, and their sum provides burn total PM emissions, E_{burn} = 76.4 g PM. Substituting FW_{burn} and E_{burn} into equation 11 yields $EFPM_{burn}$ = 2.2 g PM per kg firewood used. Figure 18 shows FW_{burn}, FC_{burn} (FC for the model burn), and E_{burn} by fire phase for the model burn with MC = 20 percent. Most (78%) of the 12.4 kg of firewood input during the burnup phase is carried over to the steady phase (green shading in fig. 18a). The majority of firewood consumption (cross-hatched area of top panel in fig. 18) occurs during the steady phase (55%), however, consumption in the burndown phase is significant (37%). Given the amount of firewood used in fire pits like those tested in our study, $EFPM_{burn}$ derived from the baseline model burn may be used to calculate total EPM. An example of such an emission calculation used to estimate annual PM emissions from low-smoke fire pits is demonstrated in section 4.2

Our fire pit testing showed differences in EFPM across fire phases (section 3), for a given MC EFPM decreased as the fires progressed, being consistently highest for the burnup phase and lowest for burndown phase (fig. 10). For each phase, our testing also quantified the dependence of EFPM and CC on MC. Increasing MC increased EFPM (table 8, fig. 12) and decreased CC (table 11, fig. 17). The effect of MC on FC and EPM for the model burn is shown in figure 19. Increasing the MC reduces burnup and steady phase CC and shifts FC into the burndown phase. For the baseline model burn, increasing MC from 10 percent to 30 percent decreases burnup phase FC by 44 percent (1.6 kg), decreases steady phase FC by 23 percent (7.4 kg), and increases burndown phase FC by 59 percent (5.7 kg). Despite the net shift of FC to the burndown phase, which has the lowest EFPM at a given MC, burn total EPM increases 35 percent (from 65 g to 88 g) due to the positive EFPM response to MC increasing from 10 percent to 30 percent—$EFPM_{burn}$ increases from 1.8 g kg^{-1} to 2.5 g kg^{-1}.

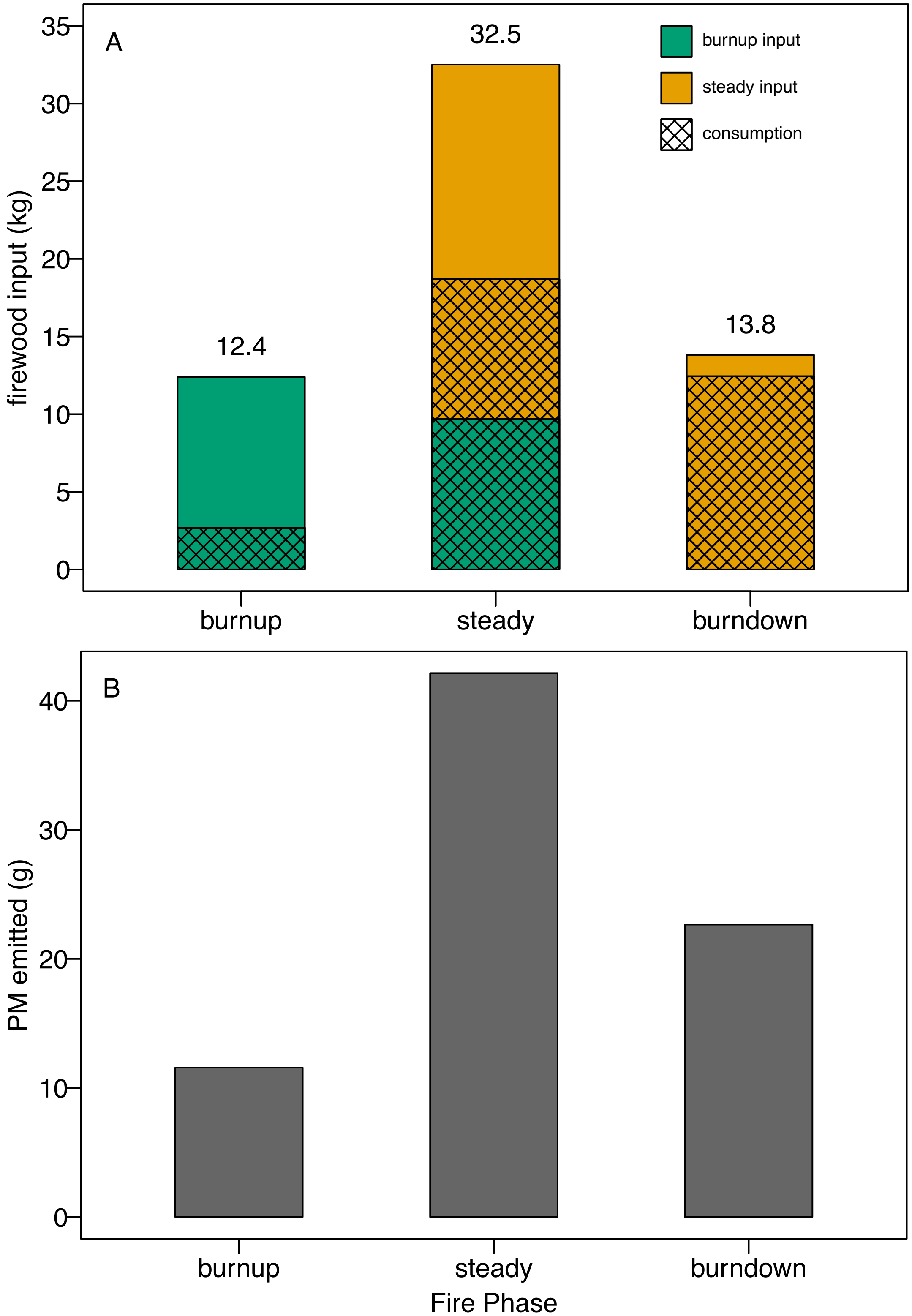

Figure 18—Results for model burn. (A) Firewood input, carry over and consumption by fire phase (dry weight). Green and orange filling are firewood input during burnup and steady phases, respectively. Cross hatching denotes fuel consumed. (B) PM emitted by fire phase.

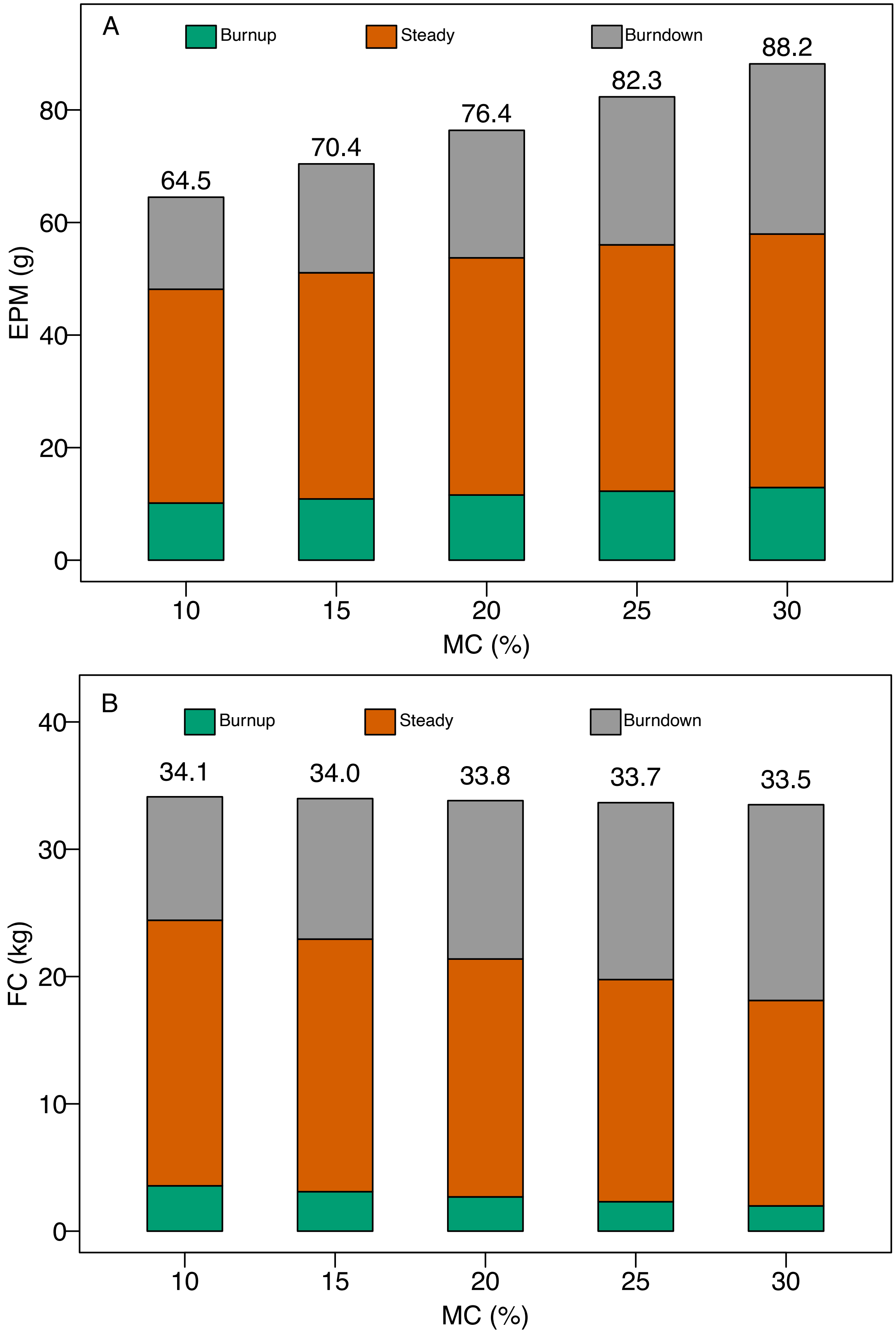

Figure 19—Model burn (A) PM emitted and (B) fuel consumption by fire phase versus MC.

To illustrate the effect of the duration of the steady and burndown phases, we ran three burn scenarios for a range of MC: (1) steady phase burn duration (t_{sb}) of 120 minutes and the fire allowed to smolder to extinction; (2) steady phase burn duration (t_{sb}) of 240 minutes and the fire allowed to smolder to extinction; and (3) steady phase burn duration (t_{sb}) of 120 minutes and the fire extinguished 60 minutes into the burndown phase. Burn integrated FC, EPM, and $EFPM_{burn}$ for the three scenarios are provided in table 14, and $EFPM_{burn}$ is plotted versus MC in figure 20. Increasing the steady phase duration, i.e. assuming a longer average burn duration, increases the per burn firewood use, FW_{burn}, and E_{burn}, but has little impact on the $EFPM_{burn}$ (fig. 20a). However, our assumption that users will allow the fire pit to smolder to extinction and that extinction occurs when 90 percent of the firewood present at the start of the burndown phase has been consumed is more impactful. For example, if it is assumed that users extinguish the fire 60 minutes into the burndown phase (scenario 3, figure 20b) instead of allowing the fire to burn to extinction, which takes 89 minutes for a 120-minute steady burn phase and MC=20 percent, FC_{burn} and EPM are reduced. Hence, $EFPM_{burn}$ are reduced by 10–15 percent at the higher MC values as compared with the baseline model in which the fire is assumed to smolder to extinction (fig. 20b).

We must emphasize a few key limits of our burn model. First, it is applicable only to the fire pits tested in this study or fire pits expected to behave in a similar manner (e.g., due to similarity of design). Second, the model assumes the use of split hardwood logs and a user fueling cycle—temporal spacing and mass of firewood inputs—resembling that used in our testing. Perhaps most importantly the model burn does not consider how user desire for radiant heat from the fire pit will be a factor in the fueling rate, and this may impact $EFPM_{burn}$.

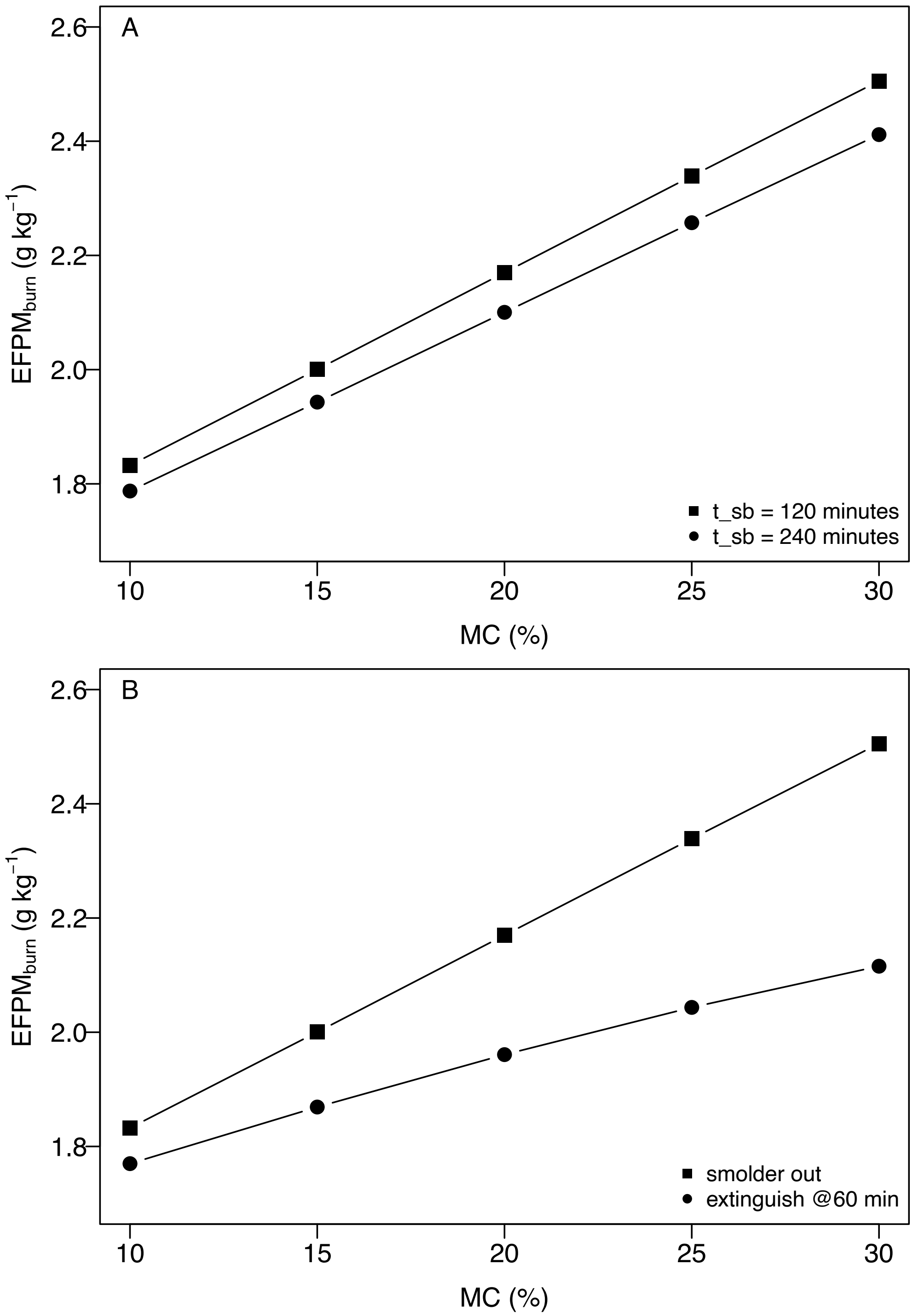

Figure 20—Model burn EFPM burn for (A) scenario 1: steady phase burn duration (t_{sb}) of 120 minutes and the fire allowed to smolder to extinction and scenario 2: steady phase burn duration (t_{sb}) of 240 minutes and the fire allowed to smolder to extinction. (B) scenario 1: steady phase burn duration (t_{sb}) of 120 minutes and the fire allowed to smolder to extinction, and scenario 3: steady phase burn duration (t_{sb}) of 120 minutes and the fire extinguished 60 minutes into the burndown phase.

4.2 Example Emission Inventory Calculation

In this section we demonstrate how our model burn can be used to calculate emission inventories from residential wood combustion activity data. The MPCA conducts comprehensive statewide surveys of residential wood combustion, and their analysis of these surveys produces estimates of the annual volume of firewood used in outdoor recreational equipment (ORE). The ORE class (which is SCC code 2104008700) includes fire pits, fire rings, chimeneas, etc. The following calculations and discussion are intended to (1) illustrate how our testing results may be applied to estimate EPM from outdoor recreational fire pit use and (2) demonstrate the potential impact low-smoke fire pit usage could have on state level ORE emission estimates.

The 2021 MPCA survey (Kuhl-Stennes et al. 2022) estimates that statewide 430,000 cords of firewood were burned in 930,000 pieces of ORE (0.46 cords $piece^{-1}$). Assuming an average firewood species distribution of like that used in our emissions testing (around one-third of each red oak, birch, and maple), wood species densities can be combined with firewood volume to estimate the mass (dry-weight) of firewood used. The species weighted density is 533 kg m^{-3} based on specific gravities for northern red oak, yellow birch, and maple (dry-weight mass and green volume; Green et al. 1999). The volume of a cord is 3.62 m^3, however this includes airspace, which due to the irregular shape of split wood, can account for up to 40 percent of the total cord volume. A net cord, the volume of actual wood present in a cord, is usually between 2.27 m^3 and 2.83 m^3; we assume an average net cord volume of 2.55 m^3. The species-weighted density and net cord volume yield a cord mass (oven-dry) of 1,359 kg $cord^{-1}$ and total mass of firewood used in ORE of 584,370 metric ton (1 metric ton = 1000 kg). Annual PM emitted from ORE may be calculated as:

$$EPM = FW((1-\alpha)EFPM_{NEI} + \alpha EFPM_{burn}) \qquad (12)$$

where (1) EPM is the mass of $PM_{2.5}$ emitted (g), (2) FW is the dry mass of firewood used (kg), (3) α is the fraction of firewood used in low-smoke fire pits, (4) $EFPM_{NEI}$ is the USEPA NEI $PM_{2.5}$ emission factor (11.3 g kg^{-1}; section 3.3) for ORE, and (5) $EFPM_{burn}$ is the $PM_{2.5}$ emission factor for our baseline model burn (table 13) for MC = 20 percent (2.2 g PM per kg firewood used). The uncertainty in this calculation associated with MC, assumed to be 20 percent, is ±16 percent if the actual MC were 10 percent or 30 percent (see figure 20).

The 2021 MPCA RWC survey does not provide data for estimating the fraction of firewood used in specific ORE types, such as low-smoke fire pits. Assuming firewood use was spread evenly across the ORE pieces, we calculate EPM for different levels of low-smoke fire pit usage (α in equation 12). Figure 21 plots EPM for different levels of low-smoke fire pit usage with total FW = 584,370 metric tons based on the MPCA RWC survey as detailed above. When all ORE are assumed to be conventional devices for which $EFPM_{NEI}$ is a reasonable estimate, annual EPM is 6,604 metric tons. Emissions decrease rapidly as the share of low-smoke fire pits increases owing to the large difference in EFPM for the device types: $EFPM_{burn}/EFPM_{NEI} = 0.20$. Based on the MPCA survey estimates that 930,000 pieces of ORE were active statewide in 2021, average annual firewood use is 628 kg piece^{-1} with PM emissions of ~7.1 kg piece^{-1} using $EFPM_{NEI}$. This implies an annual reduction of ~5.7 kg PM for each conventional ORE piece that is replaced by a low-smoke fire pit (assuming the NEI EPM (table 10) is an accurate estimate for conventional ORE).

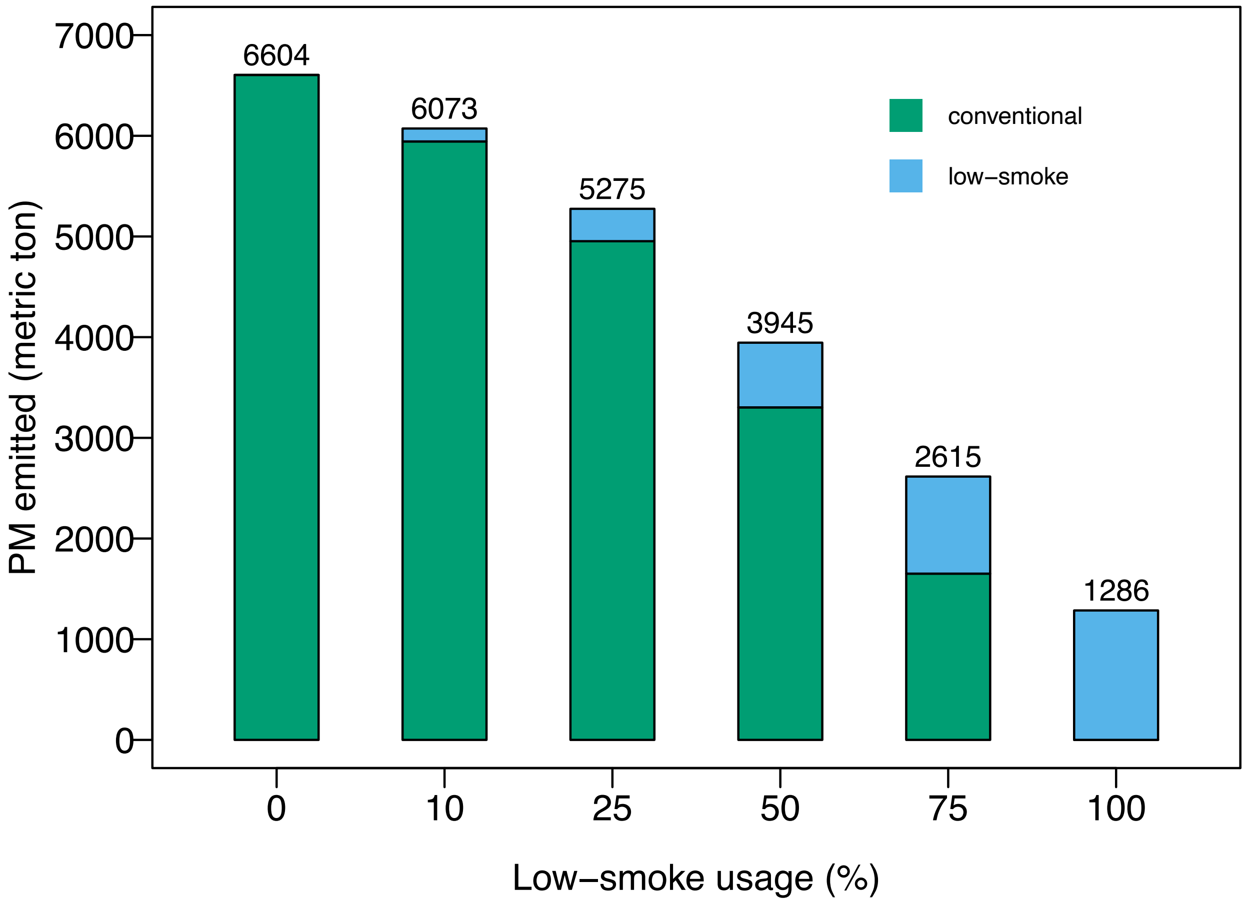

Figure 21—Annual PM emissions, based on firewood use from MPCA RWC Survey, for different levels of low-smoke fire pit usage.

5. Conclusion

EFPM, $EFCH_4$, EFCO, and $EFCO_2$, FW, and CC were measured for three outdoor recreational fire pits operated using a burn-cycle designed to simulate typical recreational use. The three fire pits tested—Solo, Breeo, and Pilot, were of a similar barrel design, with the Solo and Breeo specifically designed as low-smoke alternatives to traditional fire pits. The burn-cycle consisted of three phases: burnup, steady, and burndown, with the steady phase representing the primary mode for recreational use. The measurements of EFs and CC were analyzed using burn phase specific GLMMs which were used to predict burn phase specific MC-dependent EFs and CC for the average low-smoke fire pit for MC 10 percent–30 percent. Steady phase EFPM for the average low-smoke fire pit was estimated as EFPM = 2.3 (2.0, 2.5) g kg^{-1} (values in parentheses are 95 percent confidence intervals) at the benchmark MC of 20 percent. The EFPM measured in our testing (2.3 g kg^{-1}) was 80 percent lower than EFPM_NEI (11.3 g kg^{-1}), the PM EF used in the USEPA NEI.

Thus, our study confirmed that the fire pits tested produce significantly less PM (per mass of firewood consumed) than traditional fire pits or fire rings, assuming the EFPM_NEI reasonably characterizes the latter wood burning appliances. Our findings also indicate that the NEI may overestimate fire pit PM emissions, with the magnitude of the overestimate depending on the amount of outdoor recreational burning that uses fire pits like those tested in our study.

To demonstrate the utility of our test results, we constructed a model burn and calculated $EFPM_{burn}$: the burn average mass of PM emitted relative to the mass of firewood used (g PM emitted per kg firewood used (dry-weight mass)). We applied our burn model and $EFPM_{burn}$ to MPCA 2021 RWC firewood use survey data for the State of Minnesota. We found that, for each traditional fire pit (with EFPM_NEI) replaced with a low-smoke fire pit ($EFPM_{burn}$), annual PM emissions would be reduced by approximately 5.7 kg (this number is specific to firewood use data from the MPCA RWA survey). The MPCA RWC survey estimated 930,000 outdoor recreational wood burning devices were in use in 2021. This analysis indicates that replacing 25 percent of traditional fire pits in Minnesota with low-smoke versions could reduce annual PM emissions by approximately 1,300 metric tons.

We emphasize that our test results and model burn are applicable only to the fire pits tested in this study or fire pits expected to behave in a similar manner (e.g., due to similarity of design). Further, the model burn assumes the use of split hardwood logs and a user fueling cycle—temporal spacing and mass of firewood inputs—resembling that used in our testing. Finally, the model burn does not consider how user desire for radiant heat from the fire pit will be a factor in the fueling rate and how it might impact $EFPM_{burn}$.

References

Akagi, S.K.; Yokelson, R.J.; Wiedinmyer, C.; [et al.]. 2011. Emission factors for open and domestic biomass burning for use in atmospheric models. Atmos. Chem. Phys. 11(9): 4039-4072. Doi:10.5194/acp-11-4039-2011.

American Society of Landscape Architects. 2018. ASLA Survey: Demand high for residential landscapes with sustainability and active living elements. [Last Updated 03 April 2018]. https://www.asla.org/NewsReleaseDetails.aspx?id=62172 [Accessed 16 October 2023]

Aurell, J.; Gullett, B.K.; Tabor, D.; [et al.]. 2017. Emissions from prescribed burning of timber slash piles in Oregon. Atmospheric Environment. 150: 395-406. 10.1016/j.atmosenv.2016.11.034.

Brooks, M.E.; Kristensen, K.; van Benthem, K.J.; [et al.]. 2017. glmmTMB balances speed and flexibility among packages for zero-inflated generalized linear mixed modeling. The R Journal. 9(2): 378-400 10.32614/RJ-2017-066.

Christian, T.J.; Kleiss, B.; Yokelson, R.J.; [et al.]. 2004. Comprehensive laboratory measurements of biomass-burning emissions: 2. First intercomparison of open-path FTIR, PTR-MS, and GC-MS/FID/ECD. Journal of Geophysical Research: Atmospheres. 109(D2). 10.1029/2003jd003874.

Grand View Research. 2024. North America fire pits market size, share & trends analysis report by product (wood burning, propane, charcoal, gas), by type, by application (indoor, outdoor), by sales channel (B2B, B2C), by region, and segment forecasts, 2025–2030. Report ID: GVR-4-68040-103-1. https://www.grandviewresearch.com/industry-analysis/north-america-fire-pits-market-report Accessed 31 March 2025.

Green, D.W.; Winandy, J.E.; Kretschmann, D.E.; 1999. Mechanical properties of wood. Wood handbook: Wood as an engineering material. Madison, WI: U.S. Department of Agriculture, Forest Service, Forest Products Laboratory. 4-1, 4-45.

Hartig, F. 2022. DHARMa: residual diagnostics for hierarchical (multi-level / mixed) regression models. R package version 0.4.6. https://CRAN.R-project.org/package=DHARMa

Hosseini, S.; Li, Q.; Cocker, D; [et al.]. 2010. Particle size distributions from laboratory-scale biomass fires using fast response instruments. Atmospheric Chemistry and Physics. 10(16): 8065-8076. https://doi.org/10.5194/acp-10-8065-2010

Houck, J.; Crouch, J; Huntley, R. 2001. Review of wood heater and fireplace emission factors. Technical presentation at the International Emission Inventory Conference, One Atmosphere, One Inventory, Many Challenges. Denver, CO. https://gaftp.epa.gov/Air/nei/ei_conference/EI10/pm/houck.pdf

Houck, J.E.; Eagle, B.N. 2006. Task 6 Technical Memorandum 4 (Final Report): Control Analysis and Documentation for Residential Wood Combustion in the MANE-VU Region, Mid-Atlantic Regional Air Management Association, Inc.

Huddleston, T.; Rega, S. 2023. How two Texan brothers 'reinvented fire' to build a $400 million backyard campfire company with a cult following. CNBC [Published 14 February 2023]. https://www.cnbc.com/2023/02/14/how-solo-stove-became-a-400-million-fire-pit-company-cult-following.html [Accessed 16 October 2023].

Jimenez, D.; Forthofer, J.; Reardon, J; [et al.]. 2007. Fire behavior sensor package remote trigger design. In: Butler, Bret W.; Cook, Wayne, comps. The fire environment--innovations, management, and policy; conference proceedings., 26-30 March 2007; Destin, FL. Proceedings RMRS-P-46CD. Fort Collins, CO: U.S. Department of Agriculture, Forest Service, Rocky Mountain Research Station. CD-ROM. p. 499-505.

Kramer, C.Y. 1956. Extension of Multiple Range Tests to Group Means with Unequal Numbers of Replications, Biometrics 12:307–310.

Krug, J.; Long, R.; Colón, M.; [et al.]. 2021. Evaluation of small form factor, filter-based PM (2.5) samplers for temporary non-regulatory monitoring during wildland fire smoke events. Atmos Environ 265(3): 118718. https://doi.org/10.1016/j.atmosenv.2021.118718

Kuhl-Stennes, M.; Field, H.S.; Jackson, A. 2019. 2018 Residential Wood Combustion Survey. Saint Paul, MN, Minnesota Pollution Control Agency. https://www.pca.state.mn.us/sites/default/files/aq-ei4-47.pdf [Accessed 16 October 2023].

Kuhl-Stennes, M.; Jackson, A.; Kovacevic, A. 2022. 2020 Residential Wood Combustion Survey. Saint Paul, MN, Minnesota Pollution Control Agency. https://www.pca.state.mn.us/sites/default/files/aq-ei4-48.pdf [Accessed 16 October 2023].

Lemieux, P.M.; Lutes, C.C.; Santoianni, D.A. 2004. Emissions of organic air toxics from open burning: a comprehensive review. Progress in Energy and Combustion Science 30(1): 1-32. https://doi.org/10.1016/j.pecs.2003.08.001

Lenth, R. 2024. emmeans: Estimated Marginal Means, aka Least-Squares Means. R package version 1.10.4, https://CRAN.R-project.org/package=emmeans

McMeeking, G.R.; Kreidenweis, S.M.; Baker, S.; [et al.]. 2009. Emissions of trace gases and aerosols during the open combustion of biomass in the laboratory. Journal of Geophysical Research: Atmospheres 114(D19). doi:10.1029/2009jd011836.

Ottmar, R.D. 2014. Wildland fire emissions, carbon, and climate: Modeling fuel consumption. Forest Ecology and Management 317: 41-50.

Prichard, S.J.; Rowell, E.M.; Hudak, A. T.; [et al.]. 2022. Fuels and Consumption. Wildland Fire Smoke in the United States: A Scientific Assessment. D. L. Peterson, S. M. McCaffrey and T. Patel-Weynand. Cham, Springer International Publishing: 11-49.

R Core Team. 2024. R: A Language and Environment for Statistical Computing. R Foundation for Statistical Computing, Vienna, Austria. https://www.R-project.org

Reid, J.S.; Koppmann, R.; Eck, T.F.; [et al.]. 2005. A review of biomass burning emissions part II: intensive physical properties of biomass burning particles. Atmos. Chem. Phys. 5(3): 799-825. https://doi.org/10.5194/acp-5-799-2005

Urbanski, S.P. 2013. Combustion efficiency and emission factors for wildfire-season fires in mixed conifer forests of the northern Rocky Mountains, US. Atmos. Chem. Phys. 13(14): 7241-7262. https://doi.org/10.5194/acp-13-7241-2013

Urbanski, S.P. 2014. Wildland fire emissions, carbon, and climate: Emission factors. Forest Ecology and Management 317: 51-60. https://doi.org/10.1016/j.foreco.2013.05.045

Urbanski, S.P.; O'Neill, S.M.; Holder, A.L.; [et al.]. 2022. Emissions. In: Peterson, David L.; McCaffrey, Sarah M.; Patel-Weynand, Toral, eds. 2022. Wildland Fire Smoke in the United States: A Scientific Assessment. Cham, Switzerland: Springer Nature Switzerland AG. 121-165. Chapter 5. https://doi.org/10.1007/978-3-030-87045-4_5

U.S. Environmental Protection Agency [USEPA]. 2019. Integrated Science Assessment (ISA) for Particulate Matter (Final Report, Dec 2019). U.S. Environmental Protection Agency, Washington, DC, EPA/600/R-19/188. from https://cfpub.epa.gov/ncea/isa/recordisplay.cfm?deid=347534

U.S. Environmental Protection Agency [USEPA]. 2021. Comparative Assessment of the Impacts of Prescribed Fire Versus Wildfire (CAIF): A Case Study in the Western U.S. U.S. Environmental Protection Agency, Washington, DC, EPA/600/R-21/197. from https://cfpub.epa.gov/ncea/risk/recordisplay.cfm?deid=352824

U.S. Environmental Protection Agency [USEPA]. 2022. Other Test Method 48 (OTM-48): Emission Factor Determination by the Carbon Balance. U.S. Environmental Protection Agency, Washington, DC. from https://www.epa.gov/emc/emc-other-test-methods

U.S. Environmental Protection Agency [USEPA]. 2023a. Wood Smoke and Your Health. [Last Updated 18 August 2023] https://www.epa.gov/burnwise/wood-smoke-and-your-health [Accessed 16 October 2023].

U.S. Environmental Protection Agency [USEPA]. 2023b. 2020 National Emissions Inventory (NEI) Data. 2020 NEI Data and Documentation. [last Updated 28 February 2025]. https://www.epa.gov/air-emissions-inventories/2020-national-emissions-inventory-nei-data [Accessed 16 October 2023].

Yokelson, R.J.; Griffith, D.W.T.; Ward, D.E. 1996. Open-path Fourier transform infrared studies of large-scale laboratory biomass fires. Journal of Geophysical Research: Atmospheres 101(D15): 21067-21080. doi:10.1029/96JD01800

Appendix A—Gap Filling Missing CRDS Data

During round 3 of testing, a recurring software malfunction that began during burn number 6 (BurnID = 2021061506) and persisted through burn number 10 (BurnID = 2021062110) resulted in periodic losses of CRDS data (CO_2, CO, CH_4). Virtually no data was lost during the burnup phase because the software was restarted prior to each burn and the malfunction typically surfaced after approximately 25 minutes or more of operation. The malfunction completely subsided for the final two burns of round 3 testing. To partially compensate for the periodic CRDS data losses, the LI-COR CO_2 instrument that was deployed on the chamber floor to monitor background CO_2 was redeployed to the sampling platform beginning with burn number 8 (BurnID = 2021061708). We note that the LI-COR measurements taken on the chamber floor during the preceding 24 burns demonstrated that fluctuations in the background CO_2 were too small to significantly affect the measured ΔX and calculated EFX.

The LI-COR was calibrated *versus* the CRDS and its measurements were used to gap fill missing CRDS CO_2. The LI-COR data allowed us to calculate EFPM using only carbon from CO_2 and PM (EFPM*) in the denominator of Eq. 1 ($\Delta C = \Delta C_{CO_2} + \Delta C_{CO} + \Delta C_{CH_4} + \Delta C_{PM}$). To assess the impact of neglecting carbon CO and CH_4 in EFPM calculations we compared EFPM versus EFPM* for the 26 burns with complete CRDS data. Figure A.1 plots steady and burndown phase EFPM *versus* EFPM* with the best-fit parameters and R^2 for linear least squares regression models. As expected, neglecting the contribution of CO and CH_4 in calculating EFPM has a small effect—EFPM* overestimates EFPM by ~5% and ~7%, for the steady and burndown phase, respectively.

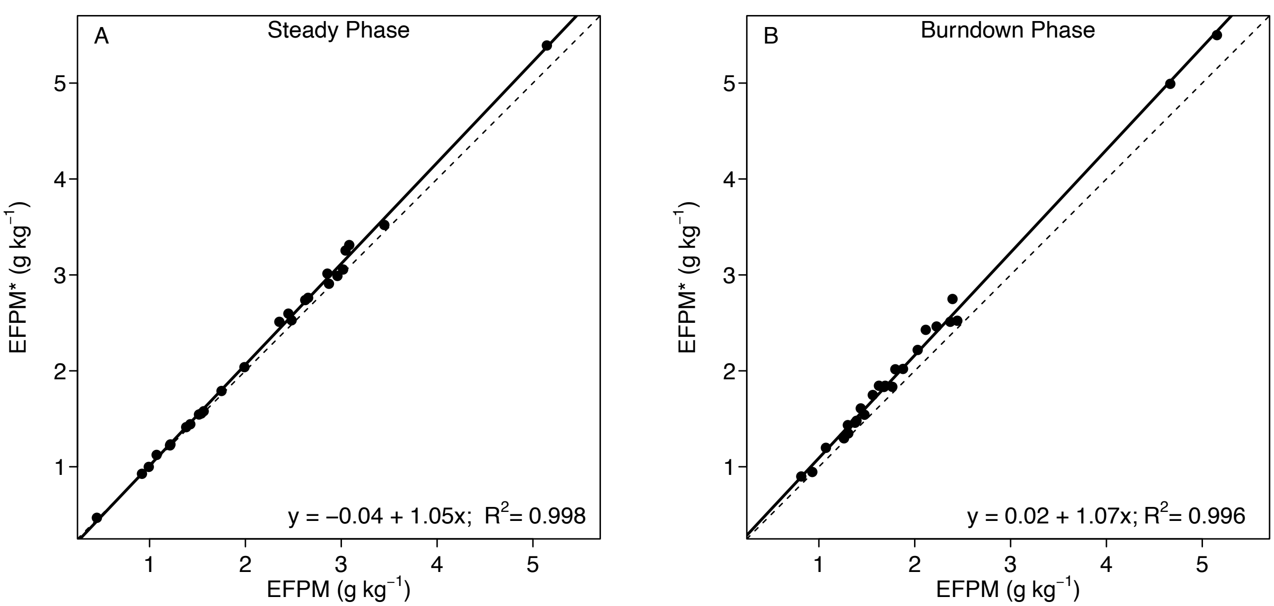

Figure A.1—The EFPM plotted versus EFPM* (EFPM calculated using carbon from only CO_2 and PM in the denominator of Eq. 1 with linear least squares regression model (solid line) and 1:1 line (dashed line). (A) Steady phase and (B) burndown phase.

Appendix B—Test Results by Phase for all Burns

Table B.1—Burn phase specific emission factors (EF) for PM, CO_2, CO, CH_4, PM*; carbon emitted (C_{tot}), radiant heat flux (RF), firewood consumed (FC), combustion completeness (CC; section 2.4) and excess PM mass mixing ratio. The EFPM* is EFPM calculated considering only the carbon emitted as CO_2 and PM (Appendix A).

BurnID	Fire pit	Phase	t_{dur} s	MC (%)	EFPM g kg^{-1}	$EFCO_2$ g kg^{-1}	EFCO g kg^{-1}	$EFCH_4$ g kg^{-1}	C_{tot} mgC m^{-3}	EFPM* g kg^{-1}	RF W m^{-2}	FC kg	CC	ΔPM mg m^{-3}
2019050803	Solo	burnup	1510	27	3.73	1777	27.9	1.14	170.8	3.83	283	2.69	0.23	1.276
2019050803	Solo	steady	4430	27	1.52	1795	21.0	0.75	360.4	1.54	1316	16.64	0.79	1.095
2019050803	Solo	burndown	1340	27	0.82	1663	103.8	2.05	224.9	0.90	652	3.14	0.71	0.367
2019050804	Breeo	burnup	1850	21	7.52	1730	49.9	2.30	139.1	7.89	207	3.15	0.22	2.093
2019050804	Breeo	steady	4400	21	2.35	1717	63.4	3.86	247.2	2.51	757	13.30	0.68	1.186
2019050804	Breeo	burndown	1290	21	1.68	1676	91.2	3.58	176.6	1.83	576	2.79	0.45	0.593
2019050905	Breeo	burnup	1740	24	5.48	1742	45.3	2.45	154.0	5.72	353	3.45	0.23	1.688
2019050905	Breeo	steady	4210	24	2.86	1729	55.9	3.56	232.8	3.01	825	12.61	0.65	0.837
2019050905	Breeo	burndown	1280	24	2.03	1674	93.3	2.97	166.9	2.22	555	2.75	0.40	0.678
2019050906	Solo	burnup	1760	11	1.68	1801	16.8	0.65	222.6	1.71	684	4.54	0.26	0.749
2019050906	Solo	steady	4170	11	1.38	1789	24.9	0.71	357.4	1.41	1749	17.26	0.77	0.993
2019050906	Solo	burndown	1350	11	1.80	1630	121.6	2.77	205.0	2.02	903	3.20	0.61	0.737
2019051007	Breeo	burnup	1710	13	9.41	1699	64.2	3.69	118.9	10.01	118	2.48	0.16	2.236
2019051007	Breeo	steady	4320	13	3.08	1742	47.1	3.61	261.3	3.31	768	13.75	0.71	1.594
2019051007	Breeo	burndown	1240	13	1.30	1661	99.8	4.39	159.4	1.43	467	2.41	0.42	0.415
2019051008	Solo	burnup	1760	14	1.87	1813	9.7	0.32	431.5	1.88	1794	7.67	0.44	1.610
2019051008	Solo	steady	4030	14	1.07	1746	51.5	1.29	383.2	1.12	1836	15.59	0.71	0.829
2019051008	Solo	burndown	1570	14	1.07	1640	112.6	4.93	194.8	1.20	540	3.09	0.49	0.418
2019051309	Breeo	burnup	1860	10	3.35	1739	49.2	3.20	216.5	3.51	460	4.54	0.29	1.450
2019051309	Breeo	steady	3900	10	0.45	1771	34.8	2.30	263.9	0.47	1006	11.60	0.67	0.255

Table B.1 continued.

BurnID	Fire pit	Phase	t_{dur} s	MC (%)	EFPM g kg^{-1}	EFCO$_2$ g kg^{-1}	EFCO g kg^{-1}	EFCH$_4$ g kg^{-1}	C_{tot} mgC m^{-3}	EFPM* g kg^{-1}	RF W m^{-2}	FC kg	CC	ΔPM mg m^{-3}
2019051309	Breeo	burndown	1570	10	2.23	1653	105.7	3.07	163.8	2.46	615	2.90	0.50	0.730
2019051310	Pilot	burnup	1830	18	3.44	1774	29.5	1.61	224.5	3.54	480	4.57	0.32	1.547
2019051310	Pilot	steady	4040	18	3.04	1720	61.3	3.47	214.3	3.25	729	9.62	0.64	1.176
2019051310	Pilot	burndown	1330	18	1.63	1612	128.4	5.49	147.3	1.84	504	2.18	0.40	0.479
2019051411	Pilot	burnup	1850	14	2.29	1781	27.3	1.47	241.5	2.35	532	5.03	0.33	1.104
2019051411	Pilot	steady	4020	14	2.45	1727	57.1	3.79	228.0	2.60	801	10.31	0.60	1.054
2019051411	Pilot	burndown	1330	14	1.44	1634	114.7	5.58	169.1	1.61	825	2.53	0.37	0.486
2019120901	Breeo	burnup	1500	9	2.10	1805	14.2	0.45	204.9	2.13	n.d.	3.38	0.27	0.862
2019120901	Breeo	steady	4230	9	1.54	1811	11.2	0.38	351.5	1.55	n.d.	16.37	0.70	1.082
2019120901	Breeo	burndown	1480	9	1.88	1700	79.2	1.70	207.9	2.02	n.d.	3.39	0.48	0.781
2019121002	Breeo	burnup	1500	9	1.36	1811	11.5	0.43	296.1	1.38	1356	5.22	0.43	0.808
2019121002	Breeo	steady	4050	9	1.21	1816	8.8	0.23	298.1	1.22	1938	14.19	0.62	0.723
2019121002	Breeo	burndown	1660	9	1.31	1775	33.8	0.85	216.3	1.35	1226	4.22	0.49	0.565
2019121103	Solo	burnup	1650	7	2.78	1812	8.8	0.18	287.8	2.80	1282	5.04	0.34	1.601
2019121103	Solo	steady	4050	7	2.96	1808	11.2	0.11	440.4	2.99	3916	18.92	0.75	2.607
2019121103	Solo	burndown	1510	7	1.56	1635	122.2	0.94	243.8	1.75	1825	3.91	0.63	0.762
2019121104	Solo	burnup	1650	6	2.14	1813	9.4	0.21	267.2	2.16	1158	5.00	0.29	1.143
2019121104	Solo	steady	4050	6	2.87	1804	14.1	0.20	479.0	2.91	4380	22.01	0.76	2.751
2019121104	Solo	burndown	1510	6	2.39	1591	149.3	0.72	268.4	2.75	2063	4.60	0.68	1.285
2019121205	Solo	burnup	1650	8	1.91	1817	7.1	0.14	329.0	1.93	1687	6.14	0.36	1.260
2019121205	Solo	steady	4050	8	3.02	1804	13.8	0.20	469.6	3.06	4317	21.52	0.76	2.836
2019121205	Solo	burndown	910	8	2.37	1725	63.5	1.05	324.5	2.51	2593	3.34	0.49	1.538
2019121306	Breeo	burnup	1350	8	1.88	1800	16.9	0.68	289.1	1.91	934	4.48	0.28	1.086

Table B.1 continued.

BurnID	Fire pit	Phase	t_{dur} s	MC (%)	EFPM g kg^{-1}	EFCO$_2$ g kg^{-1}	EFCO g kg^{-1}	EFCH$_4$ g kg^{-1}	C_{tot} mgC m^{-3}	EFPM* g kg^{-1}	RF W m^{-2}	FC kg	CC	ΔPM mg m^{-3}
2019121306	Breeo	steady	3150	8	0.92	1819	6.9	0.27	356.0	0.93	2119	12.87	0.62	0.656
2019121306	Breeo	burndown	1510	8	1.39	1723	65.4	1.65	189.7	1.48	1035	3.29	0.42	0.528
2019121607	Pilot	burnup	600	8	2.74	1789	22.6	0.85	235.1	2.80	1410	1.81	0.23	1.289
2019121607	Pilot	steady	3900	8	1.42	1806	13.8	0.64	329.6	1.44	3362	16.50	0.70	0.939
2019121607	Pilot	burndown	1510	8	1.69	1678	92.6	2.08	177.3	1.84	2889	3.44	0.48	0.600
2019121708	Pilot	burnup	1350	8	2.46	1797	18.1	0.71	228.3	2.50	1134	3.34	0.22	1.124
2019121708	Pilot	steady	3150	8	1.22	1808	13.0	0.68	359.3	1.23	3273	12.27	0.50	0.875
2019121708	Pilot	burndown	1510	8	1.77	1762	40.1	1.52	223.0	1.83	2994	3.65	0.30	0.788
2019121809	Solo	burnup	1350	9	2.71	1815	7.3	0.18	337.1	2.73	2808	5.03	0.34	1.829
2019121809	Solo	steady	3150	9	3.45	1788	22.6	0.51	463.5	3.52	5482	16.14	0.73	3.198
2019121809	Solo	burndown	1510	9	2.12	1592	147.3	1.61	218.7	2.43	2112	3.65	0.62	0.925
2019121910	Breeo	burnup	1350	8	1.74	1807	13.5	0.48	252.5	1.76	1295	4.36	0.30	0.878
2019121910	Breeo	steady	3150	8	0.99	1818	7.5	0.28	342.7	1.00	2799	13.79	0.62	0.680
2019121910	Breeo	burndown	1510	8	1.38	1727	62.2	1.82	171.6	1.46	1732	3.31	0.40	0.473
2021060701	Breeo	burnup	1350	28	5.41	1754	38.4	1.89	199.5	5.61	97	2.35	0.17	2.158
2021060701	Breeo	steady	3450	28	1.75	1789	23.1	1.40	360.7	1.79	341	10.84	0.49	1.263
2021060701	Breeo	burndown	1500	28	2.44	1771	33.5	1.51	267.6	2.52	271	3.49	0.31	1.308
2021060802	Breeo	burnup	1350	35	5.34	1774	27.5	1.19	165.3	5.48	108	1.41	0.11	1.767
2021060802	Breeo	steady	3450	35	5.15	1737	46.5	3.96	378.0	5.39	343	8.24	0.38	3.890
2021060802	Breeo	burndown	1500	35	1.26	1781	27.9	1.81	300.4	1.30	348	2.85	0.21	0.758
2021060903	Solo	burnup	1350	24	7.51	1747	39.7	1.99	195.9	7.80	89	2.25	0.15	2.942
2021060903	Solo	steady	3450	24	1.99	1785	25.6	1.18	374.4	2.04	307	10.96	0.47	1.490
2021060903	Solo	burndown	1740	24	1.26	1759	43.1	1.31	354.0	1.31	362	5.23	0.43	0.889

Table B.1 continued.

BurnID	Fire pit	Phase	t_{dur} s	MC (%)	EFPM g kg^{-1}	$EFCO_2$ g kg^{-1}	EFCO g kg^{-1}	$EFCH_4$ g kg^{-1}	C_{tot} mgC m^{-3}	EFPM* g kg^{-1}	RF W m^{-2}	FC kg	CC	ΔPM mg m^{-3}
2021061004	Solo	burnup	1350	25	8.21	1746	39.3	2.12	145.1	8.53	75	1.58	0.11	2.383
2021061004	Solo	steady	3450	25	2.48	1794	19.1	1.01	406.4	2.53	341	11.30	0.49	2.017
2021061004	Solo	burndown	1500	25	0.93	1804	16.4	0.59	344.7	0.95	389	4.17	0.36	0.642
2021061105	Solo	burnup	1350	14	4.29	1779	25.7	1.17	215.6	4.39	110	2.41	0.16	1.850
2021061105	Solo	steady	3450	14	1.56	1813	9.6	0.38	483.5	1.58	540	13.81	0.56	1.513
2021061105	Solo	burndown	1500	14	1.48	1751	48.1	1.25	338.8	1.54	370	4.21	0.38	1.000
2021061506	Breeo	burnup	1290	21	3.76	1782	24.9	1.02	200.3	3.85	129	2.93	0.20	1.508
2021061506	Breeo	steady	3450	21	4.48	1732	50.0	4.23	307.4	4.71	278	12.01	0.52	2.753
2021061506	Breeo	burndown	1500	21	2.25	1757	38.8	3.48	227.6	2.34	332	3.87	0.35	1.025
2021061507	Solo	burnup	1350	30	9.10	1735	48.1	n.d.	150.1	9.50	85	1.41	0.10	2.733
2021061507	Solo	steady	3450	30	1.46	1815	9.1	n.d.	541.6	1.47	607	13.05	0.58	1.583
2021061507	Solo	burndown	1500	30	1.22	1789	26.5	n.d.	368.3	1.25	476	3.86	0.41	0.900
2021061708	Breeo	burnup	1350	27	2.06	1791	21.6	1.17	346.1	2.10	255	3.92	0.28	1.425
2021061708	Breeo	steady	3450	27	1.94	1775	30.6	2.08	374.0	2.00	447	10.82	0.52	1.453
2021061708	Breeo	burndown	1500	27	1.48	1777	30.8	1.59	244.4	1.53	348	3.08	0.31	0.725
2021062109	Pilot	burnup	1350	19	5.77	1759	34.9	1.85	295.1	5.97	n.d.	3.69	0.24	3.408
2021062109	Pilot	steady	3450	19	3.25	1743	45.9	3.57	413.5	3.40	n.d.	13.23	0.58	2.687
2021062109	Pilot	burndown	1500	19	1.36	1769	35.6	1.88	270.0	1.40	n.d.	3.76	0.39	0.733
2021062110	Pilot	burnup	1350	17	4.91	1760	35.8	2.00	298.0	5.08	163	3.75	0.23	2.925
2021062110	Pilot	steady	3450	17	2.13	1783	25.6	1.91	408.1	2.18	394	13.12	0.54	1.737
2021062110	Pilot	burndown	1500	17	1.92	1761	38.7	2.55	243.4	1.99	264	3.40	0.31	0.933
2021062211	Pilot	burnup	1350	23	3.88	1769	31.5	1.79	328.4	4.00	187	2.47	0.16	2.550
2021062211	Pilot	steady	3450	23	2.62	1751	42.8	3.19	344.3	2.74	324	6.63	0.28	1.807

Table B.1 continued.

BurnID	Fire pit	Phase	t_{dur} s	MC (%)	EFPM g kg^{-1}	$EFCO_2$ g kg^{-1}	EFCO g kg^{-1}	$EFCH_4$ g kg^{-1}	C_{tot} mgC m^{-3}	EFPM* g kg^{-1}	RF W m^{-2}	FC kg	CC	ΔPM mg m^{-3}
2021062211	Pilot	burndown	1500	23	5.15	1705	65.6	4.54	203.0	5.50	192	1.70	0.10	2.092
2021062312	Pilot	burnup	1350	26	3.72	1786	22.5	1.02	231.0	3.80	168	2.03	0.14	1.717
2021062312	Pilot	steady	3450	26	2.65	1756	40.6	2.61	346.6	2.76	371	7.79	0.33	1.840
2021062312	Pilot	burndown	1500	26	4.67	1702	67.8	4.71	208.1	4.99	203	2.03	0.13	1.942

Appendix C—GLMM Results for EFPM

Table C.1—EFPM GLMM estimates for fire pit type main effects (g kg^{-1}).

Phase	Fire pit	Response	SE[a]	LCL[b]	UCL[b]
Burnup	Breeo	3.88	0.60	2.86	5.26
Burnup	Pilot	3.62	0.32	3.05	4.29
Burnup	Solo	3.85	0.37	3.19	4.66
Steady	Breeo	1.95	0.28	1.47	2.57
Steady	Pilot	2.31	0.17	2.00	2.66
Steady	Solo	2.08	0.19	1.73	2.49
Burndown	Breeo	1.71	0.11	1.51	1.94
Burndown	Pilot	2.28	0.28	1.80	2.90
Burndown	Solo	1.43	0.09	1.26	1.63

a Standard error

b Lower and upper 95 percent confidence intervals

Table C.2—EFPM GLMM contrasts for fire pit main effects.

Phase	Contrast	Ratio	SE[a]	z-ratio[b]	p-value[c]
Burnup	Breeo / Pilot	1.072	0.192	0.389	0.920
Burnup	Breeo / Solo	1.006	0.185	0.034	0.999
Burnup	Pilot / Solo	0.939	0.123	-0.485	0.879
Steady	Breeo / Pilot	0.845	0.134	-1.066	0.535
Steady	Breeo / Solo	0.936	0.159	-0.386	0.921
Steady	Pilot / Solo	1.109	0.131	0.875	0.656
Burndown	Breeo / Pilot	0.749	0.104	-2.087	0.092
Burndown	Breeo / Solo	1.194	0.110	1.924	0.132
Burndown	Pilot / Solo	1.593	0.218	3.395	0.002

a Standard error

b Wald statistic

c p-value calculated from the Wald statistic

Table C.3—EFPM GLMM estimates for fire pit type–moisture content interaction.

Phase	Fire pit	MC trend	SE[a]	LCL[b]	UCL[b]
Burnup	Breeo	0.032	0.024	-0.014	0.078
Burnup	Pilot	0.032	0.016	0.000	0.064
Burnup	Solo	0.060	0.011	0.037	0.082
Steady	Breeo	0.046	0.015	0.017	0.075
Steady	Pilot	0.037	0.016	0.006	0.069
Steady	Solo	-0.020	0.010	-0.040	0.001
Burndown	Breeo	0.008	0.008	-0.008	0.025
Burndown	Pilot	0.051	0.019	0.014	0.088
Burndown	Solo	-0.036	0.008	-0.051	-0.020

a Standard error

b Lower and upper 95 percent confidence intervals

Table C.4—EFPM GLMM contrasts for fire pit type–moisture content interaction.

Phase	Contrast	Estimate	SE[a]	z-ratio[b]	p-value[c]
Burnup	Breeo–Pilot	0.000	0.026	-0.002	1.000
Burnup	Breeo–Solo	-0.028	0.027	-1.032	0.557
Burnup	Pilot–Solo	-0.027	0.020	-1.367	0.358
Steady	Breeo–Pilot	0.009	0.020	0.441	0.898
Steady	Breeo–Solo	0.066	0.018	3.586	0.001
Steady	Pilot–Solo	0.057	0.020	2.868	0.012
Burndown	Breeo–Pilot	-0.042	0.021	-1.985	0.116
Burndown	Breeo–Solo	0.044	0.012	3.670	0.001
Burndown	Pilot–Solo	0.086	0.020	4.392	0.000

a Standard error

b Wald statistic

c p-value calculated from the Wald statistic

Appendix D—GLMM Results for $EFCH_4$

Table D.1—$EFCH_4$ GLMM estimates for fire pit main effects.

Phase	Fire pit	Response	SE[a]	LCL[b]	UCL[b]
Burnup	Breeo	1.715	0.397	1.090	2.699
Burnup	Pilot	1.451	0.209	1.095	1.924
Burnup	Solo	0.722	0.119	0.523	0.997
Steady	Breeo	2.164	0.550	1.315	3.562
Steady	Pilot	2.623	0.466	1.852	3.715
Steady	Solo	0.687	0.120	0.489	0.967
Burndown	Breeo	2.491	0.385	1.839	3.373
Burndown	Pilot	3.424	0.500	2.572	4.559
Burndown	Solo	1.724	0.335	1.178	2.523

a Standard error

b Lower and upper 95 percent confidence intervals

Table D.2—$EFCH_4$ GLMM contrasts for fire pit main effects.

Phase	Contrast	Ratio	SE[a]	z-ratio[b]	p-value[c]
Burnup	Breeo / Pilot	1.182	0.290	0.682	0.774
Burnup	Breeo / Solo	2.375	0.644	3.188	0.004
Burnup	Pilot / Solo	2.010	0.419	3.346	0.002
Steady	Breeo / Pilot	0.825	0.252	-0.630	0.804
Steady	Breeo / Solo	3.149	0.957	3.774	0.000
Steady	Pilot / Solo	3.816	0.904	5.652	0.000
Burndown	Breeo / Pilot	0.727	0.152	-1.523	0.280
Burndown	Breeo / Solo	1.445	0.353	1.504	0.289
Burndown	Pilot / Solo	1.986	0.481	2.831	0.013

a Standard error

b Wald statistic

c p-value calculated from the Wald statistic

Table D.3—EFCH$_4$ GLMM estimates for fire pit–moisture content interaction.

Phase	Fire pit	MC trend	SE[a]	LCL[b]	UCL[b]
Burnup	Breeo	-0.010	0.022	-0.053	0.034
Burnup	Pilot	0.006	0.031	-0.056	0.067
Burnup	Solo	0.100	0.024	0.054	0.146
Steady	Breeo	0.028	0.019	-0.008	0.065
Steady	Pilot	0.018	0.030	-0.040	0.076
Steady	Solo	0.037	0.022	-0.007	0.080
Burndown	Breeo	-0.013	0.017	-0.046	0.020
Burndown	Pilot	0.038	0.025	-0.012	0.087
Burndown	Solo	-0.011	0.027	-0.065	0.042

a Standard error

b Lower and upper 95 percent confidence intervals

Table D.4—EFCH$_4$ GLMM contrasts for fire pit–moisture content interaction.

Phase	Contrast	Estimate	SE[a]	z-ratio[b]	p-value[c]
Burnup	Breeo–Pilot	-0.015	0.030	-0.501	0.871
Burnup	Breeo–Solo	-0.110	0.028	-3.922	0.000
Burnup	Pilot–Solo	-0.094	0.033	-2.851	0.012
Steady	Breeo–Pilot	0.011	0.034	0.308	0.949
Steady	Breeo–Solo	-0.008	0.028	-0.294	0.953
Steady	Pilot–Solo	-0.019	0.034	-0.554	0.844
Burndown	Breeo - Pilot	-0.051	0.029	-1.779	0.177
Burndown	Breeo–Solo	-0.002	0.029	-0.055	0.998
Burndown	Pilot–Solo	0.049	0.036	1.367	0.358

a Standard error

b Wald statistic

c p-value calculated from the Wald statistic

Appendix E—GLMM Results for EFCO

Table E.1—EFCO GLMM estimates for fire pit main effect.

Phase	Fire pit	Response	SE[a]	LCL[b]	UCL[b]
Burnup	Breeo	32.9	5.8	23.3	46.5
Burnup	Pilot	28.2	2.3	24.0	33.2
Burnup	Solo	19.4	1.9	16.0	23.4
Steady	Breeo	31.7	6.9	20.7	48.5
Steady	Pilot	37.5	5.7	27.8	50.6
Steady	Solo	21.1	3.8	14.8	30.1
Burndown	Breeo	63.8	7.8	50.2	81.0
Burndown	Pilot	73.1	12.5	52.2	102.3
Burndown	Solo	76.7	11.2	57.6	102.0

a Standard error

b Lower and upper 95 percent confidence intervals

Table E.2—EFCO model contrasts for fire pit main effect.

Phase	Contrast	Ratio	SE[a]	z-ratio[b]	p-value[c]
Burnup	Breeo / Pilot	1.165	0.213	0.836	0.680
Burnup	Breeo / Solo	1.699	0.331	2.720	0.018
Burnup	Pilot / Solo	1.458	0.180	3.047	0.007
Steady	Breeo / Pilot	0.846	0.210	-0.675	0.778
Steady	Breeo / Solo	1.501	0.387	1.572	0.258
Steady	Pilot / Solo	1.775	0.398	2.560	0.028
Burndown	Breeo / Pilot	0.873	0.183	-0.649	0.793
Burndown	Breeo / Solo	0.832	0.158	-0.968	0.597
Burndown	Pilot / Solo	0.953	0.215	-0.212	0.976

a Standard error

b Wald statistic

c p-value calculated from the Wald statistic

Table E.3—EFCO GLMM estimates for fire pit type–moisture content interaction.

Phase	Fire pit	MC trend	SE[a]	LCL[b]	UCL[b]
Burnup	Breeo	-0.002	0.018	-0.037	0.034
Burnup	Pilot	0.003	0.018	-0.033	0.039
Burnup	Solo	0.070	0.011	0.048	0.091
Steady	Breeo	0.024	0.022	-0.019	0.067
Steady	Pilot	0.031	0.032	-0.032	0.094
Steady	Solo	-0.021	0.024	-0.067	0.026
Burndown	Breeo	-0.021	0.017	-0.055	0.013
Burndown	Pilot	-0.002	0.029	-0.059	0.054
Burndown	Solo	-0.049	0.017	-0.083	-0.015

a Standard error

b Lower and upper 95 percent confidence intervals.

Table E.4—EFCO model contrasts for fire pit type–moisture content interaction.

Phase	Contrast	Estimate	SE[a]	z-ratio[b]	p-value[c]
Burnup	Breeo–Pilot	-0.015	0.030	-0.501	0.871
Burnup	Breeo–Solo	-0.110	0.028	-3.922	0.000
Burnup	Pilot–Solo	-0.094	0.033	-2.851	0.012
Steady	Breeo–Pilot	0.011	0.034	0.308	0.949
Steady	Breeo–Solo	-0.008	0.028	-0.294	0.953
Steady	Pilot–Solo	-0.019	0.034	-0.554	0.844
Burndown	Breeo–Pilot	-0.051	0.029	-1.779	0.177
Burndown	Breeo–Solo	-0.002	0.029	-0.055	0.998
Burndown	Pilot–Solo	0.049	0.036	1.367	0.358

a Standard error

b Wald statistic

c p-value calculated from the Wald statistic

Appendix F—GLMM Results for $EFCO_2$

Table F.1—$EFCO_2$ GLMM estimates for fire pit main effect (kg kg^{-1}).

Phase	Fire pit	Response	SE[a]	LCL[b]	UCL[b]
Burnup	Breeo	1.77	0.012	1.75	1.79
Burnup	Pilot	1.78	0.004	1.77	1.78
Burnup	Solo	1.78	0.004	1.78	1.79
Steady	Breeo	1.77	0.008	1.76	1.79
Steady	Pilot	1.76	0.009	1.74	1.78
Steady	Solo	1.79	0.006	1.78	1.81
Burndown	Breeo	1.72	0.012	1.70	1.74
Burndown	Pilot	1.70	0.020	1.66	1.74
Burndown	Solo	1.69	0.016	1.66	1.73

a Standard error

b Lower and upper 95 percent confidence intervals

Table F.2—$EFCO_2$ GLMM contrasts for fire pit main effects.

Phase	Contrast	Ratio	SE[a]	z-ratio[b]	p-value[c]
Burnup	Breeo / Pilot	0.996	0.007	-0.584	0.829
Burnup	Breeo / Solo	0.992	0.007	-1.204	0.451
Burnup	Pilot / Solo	0.996	0.003	-1.415	0.333
Steady	Breeo / Pilot	1.007	0.007	1.017	0.566
Steady	Breeo / Solo	0.988	0.006	-2.050	0.100
Steady	Pilot / Solo	0.981	0.006	-3.131	0.005
Burndown	Breeo / Pilot	1.010	0.014	0.751	0.733
Burndown	Breeo / Solo	1.016	0.012	1.303	0.394
Burndown	Pilot / Solo	1.006	0.015	0.368	0.928

a Standard error

b Wald statistic

c p-value calculated from the Wald statistic

Table F.3—EFCO_2 model estimates for fire pit type–moisture content interaction.

Phase	Fire pit	MC trend	SE[a]	LCL[b]	UCL[b]
Burnup	Breeo	-0.001	0.001	-0.003	0.001
Burnup	Pilot	-0.001	0.000	-0.002	0.000
Burnup	Solo	-0.002	0.000	-0.002	-0.001
Steady	Breeo	-0.002	0.001	-0.003	0.000
Steady	Pilot	-0.002	0.001	-0.004	0.000
Steady	Solo	0.000	0.000	-0.001	0.001
Burndown	Breeo	0.001	0.001	0.000	0.003
Burndown	Pilot	0.000	0.002	-0.004	0.004
Burndown	Solo	0.004	0.001	0.001	0.006

a Standard error

b Lower and upper 95 percent confidence intervals.

Table F.4—EFCO_2 GLMM contrasts for fire pit type–moisture content interaction.

Phase	Contrast	Estimate	SE[a]	z-ratio[b]	p-value[c]
Burnup	Breeo - Pilot	0.000	0.001	-0.191	0.980
Burnup	Breeo - Solo	0.001	0.001	0.764	0.725
Burnup	Pilot - Solo	0.001	0.000	1.907	0.137
Steady	Breeo - Pilot	0.000	0.001	0.348	0.936
Steady	Breeo - Solo	-0.002	0.001	-2.091	0.092
Steady	Pilot - Solo	-0.002	0.001	-1.863	0.150
Burndown	Breeo - Pilot	0.001	0.002	0.705	0.761
Burndown	Breeo - Solo	-0.002	0.001	-1.507	0.288
Burndown	Pilot - Solo	-0.004	0.002	-1.612	0.241

a Standard error

b Wald statistic

c p-value calculated from the Wald statistic

Appendix G—GLMM Results for CC

Table G.1—CC GLMM estimates for fire pit main effect.

Phase	Fire pit	Response	SE[a]	LCL[b]	UCL[b]
Burnup	Breeo	0.246	0.017	0.214	0.282
Burnup	Pilot	0.232	0.020	0.195	0.273
Burnup	Solo	0.235	0.022	0.195	0.281
Steady	Breeo	0.615	0.019	0.576	0.652
Steady	Pilot	0.528	0.041	0.448	0.607
Steady	Solo	0.661	0.026	0.608	0.711
Burndown	Breeo	0.401	0.014	0.375	0.428
Burndown	Pilot	0.302	0.035	0.238	0.374
Burndown	Solo	0.519	0.033	0.454	0.584

a Standard error

b Lower and upper 95 percent confidence intervals.

Table G.2—CC GLMM contrasts for fire pit main effects.

Phase	Contrast	Odds ratio	SE[a]	z-ratio[b]	p-value[c]
Burnup	Breeo / Pilot	1.082	0.158	0.538	0.853
Burnup	Breeo / Solo	1.062	0.163	0.389	0.920
Burnup	Pilot / Solo	0.981	0.162	-0.113	0.993
Steady	Breeo / Pilot	1.428	0.257	1.976	0.118
Steady	Breeo / Solo	0.819	0.121	-1.356	0.364
Steady	Pilot / Solo	0.574	0.118	-2.709	0.018
Burndown	Breeo / Pilot	1.551	0.270	2.521	0.031
Burndown	Breeo / Solo	0.620	0.091	-3.257	0.003
Burndown	Pilot / Solo	0.400	0.086	-4.258	0.000

a Standard error

b Wald statistic

c p-value calculated from the Wald statistic

Appendix H—Histograms of Firewood Input and Consumption Rates

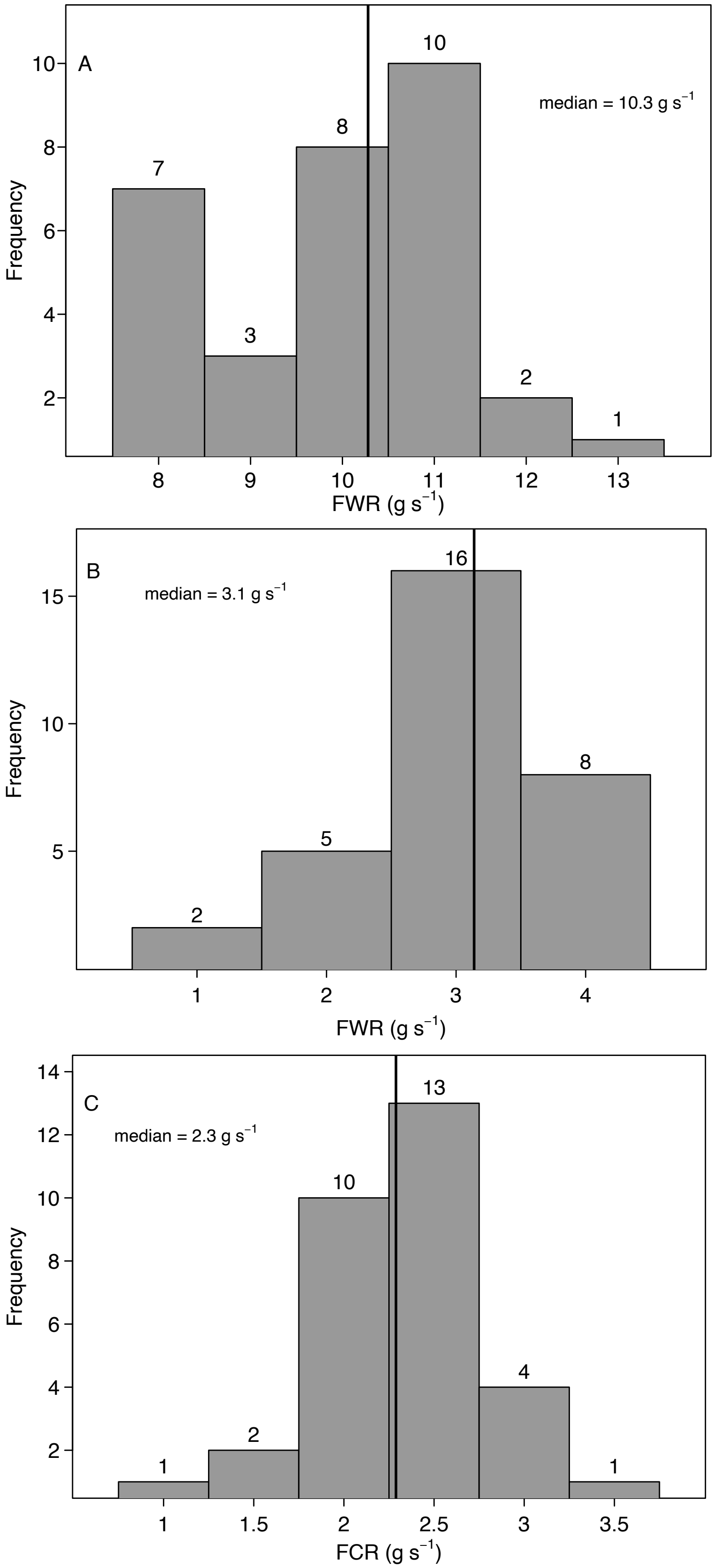

Figure H.1—Histograms of test data for (A) firewood input rate (FWR) for the burnup phase, (B) firewood input rate (FWR) for the steady phase, and (C) burndown phase firewood consumption rate (FCR). Solid lines are medians.

To learn more about RMRS publications or search our online titles:

https://research.fs.usda.gov/rmrs/products/publications

https://research.fs.usda.gov/treesearch